ACCEPTED MANUSCRIPT

https://doi.org/10.1016/j.actbio.2019.02.015

This is the Pre-Published Version.

ROCK isoforms differentially modulate cancer cell motility by mechanosensing the substrate stiffness

Yueting Peng[1], Zhongyuan Chen[1], Yu Chen[1], Shun Li[1,3], Ying Jiang[1,3], Hong Yang[1,3], Chunhui Wu[1,3], Fengming You [2], Chuan Zheng [2], Jie Zhu [2], Youhua Tan[4], Xiang Qin[1,3 *], Yiyao Liu[1,2,3 *]

[1] Department of Biophysics, School of Life Science and Technology, University of Electronic Science and Technology of China, Chengdu 610054, Sichuan, P.R. China; [2] Hospital of Chengdu University of Traditional Chinese Medicine, No. 39 Shi-er-qiao Road, Chengdu 610072, Sichuan, P.R. China; [3] Center for Information in Biology, University of Electronic Science and Technology of China, Chengdu 610054, Sichuan, P.R. China; [4] Department of Biomedical Engineering, Hong Kong Polytechnic University, Hong Kong, P.R. China

[*] To whom correspondence should be addressed:

Prof. Yiyao Liu, Ph.D

Department of Biophysics, School of Life Science and Technology, University of Electronic Science and Technology of China, Chengdu 610054, Sichuan, P. R. China. Tel: +86-28-8320-3353, fax: +86-28-8320-8238, E-mail: liuyiyao@uestc.edu.cn

or

Dr. Xiang Qin

Department of Biophysics, School of Life Science and Technology, University of Electronic Science and Technology of China. E-mail: qinxiang@uestc.edu.cn

© 2019. This manuscript version is made available under the CC-BY-NC-ND 4.0 license https://creativecommons.org/licenses/by-nc-nd/4.0/

ACCEPTED MANUSCRIPT

Abstract

Tumors are characterized by extracellular matrix (ECM) remodeling and stiffening. The importance of ECM stiffness in cancer is well known. However, the biomechanical behavior of tumor cells and the underlying mechanotransduction pathways remain unclear. Here, we used polyacrylamide (PAA) substrates to simulate tissue stiffness at different progress stages of breast cancer *in vitro*, and we observed that moderate substrate stiffness promoted breast cancer cell motility. The substrate stiffness directly activated integrin β1 and focal adhesion kinase (FAK), which accelerate focal adhesion (FA) maturation and induce the downstream cascades of intracellular signals of the RhoA/ROCK pathway. Interestingly, the differential regulatory mechanism between two ROCK isoforms (ROCK1 and ROCK2) in cell motility and mechanotransduction was clearly identified. ROCK1 phosphorylated the myosin regulatory light chain (MRLC) and facilitated the generation of traction force, while ROCK2 phosphorylated cofilin and regulated the cytoskeletal remodeling by suppressing F-actin depolymerization. The ROCK isoforms differentially regulated the pathways of RhoA/ROCK1/p-MLC and RhoA/ROCK2/p-cofilin in a coordinate fashion to modulate breast cancer cell motility in a substrate stiffness-dependent manner through integrin β1-activated FAK signaling. Our findings provide new insights into the mechanisms of matrix mechanical property-induced cancer cell migration and malignant behaviors.

***Keywords*:** ROCK isoforms; Substrate stiffness; Integrin β1; Cell motility; Mechanotransduction

ACCEPTED MANUSCRIPT

1. Introduction

Among malignant tumors, the incidence of breast cancer ranks first in women, accompanied by high death rates. Tumor metastasis is the main reason for poor prognoses and even failure of clinical treatment in patients with breast cancer [1]. Therefore, understanding and intervention of the mechanism underlying metastasis are the key steps to improve the outcome of anticancer treatments. Tumor microenvironment (TME), which consists of tumor vessels, immune cells, fibroblasts, cytokines, and the extracellular matrix (ECM), plays a key role in the initiation and progression of cancer [2]. The mechanical signals of the ECM are considered to be important components of the TME [3], such as shear stress for circulating tumor cells (CTCs) and substrate stiffness for adherent cells [4-7]. In particular, certain adherent cells can sense the substrate stiffness of ECM as a cue for regulating a variety of cellular behaviors including adhesion, morphology, locomotion, proliferation, and even differentiation of stem cells [8-10]. Although the role of substrate stiffness in fibroblasts, smooth muscle cells, and marrow-derived mesenchymal cells has been widely studied, less research currently focuses on cancer cells [11, 12]. Clinical observation found that the stiffness of tumor increased during progression, which related to tumor malignant transformation and metastasis [13, 14]. These findings suggested that mimicking the mechanical property of TME *in vitro* to uncover the mechanism of cancer malignant transformation and metastasis in cellular and molecular levels was beneficial for both

ACCEPTED MANUSCRIPT

biomechanics research and clinical applications.

To investigate how ECM stiffness influences breast cancer progression *in vitro*, an elaborate culture substrate with regulatable stiffness similar as that of normal breast or breast tumor tissue is of great necessity. Polyacrylamide (PAA) hydrogel is widely used in tissue engineering and regenerative medicine owing to its simple preparation, strong plasticity, and tunable stiffness [15]. More importantly, PAA gels are suitable for cell attachment after coating with ECM proteins. There are several kinds of ECM proteins including collagen I, collagen IV, laminin, and fibronectin [16]. These ECM proteins bind to the cell surface through integrins, which are a family of transmembrane heterodimer proteins that connect to ECM ligands extracellularly and attach to actin filaments intracellularly [17]. Among the ECM proteins, collagen I is a common collagen type that is widely distributed in different tissues and organs and interacts with integrin β1. It has been applied as a surface coating protein for several cell lines [18].

In tumor metastasis, cell migration and invasion are two critical procedures that lead to the dissemination of cancer cells from the primary tumor to distant organs. For cells to move, cytoskeletal rearrangement is required, and actin polymerization and depolymerization are performed in a coordinated manner [19, 20]. Many signaling pathways are involved in this process, and the Rho/ROCK pathway is one of the best-known mechanisms among them [21]. In brief, active Rho binds to ROCK, thereby resulting in the

ACCEPTED MANUSCRIPT

activation of myosin regulatory light chain (MRLC) and leading to actin–myosin contraction [22-24]. In addition, ROCK also phosphorylates LIM kinase and then inhibits actin depolymerization through cofilin/actin-depolymerizing factor (ADF) family proteins [25]. Focal adhesion kinase (FAK), which is required for mechanosensing and cell motility, finely regulates focal adhesion (FA) dynamics in membrane protrusion [26, 27]. After recruited by activated integrins, a positive feedback regulation between RhoA and FAK occurs in nascent FA and phosphorylated target proteins such as paxillin, along with talin [28]. Additionally, the pivotal role of FAK in breast cancer progression in mouse models was confirmed [29].

ROCK is a major downstream effector of RhoA that contributes to most processes in cancer initiation and progression. There are two ROCK isoforms, ROCK1 and ROCK2, which exhibit 90% homology in their kinase domain and 64% homology overall [30]. In a previous study, the total ROCK inhibitor Y-27632 was used to determine the role of ROCK in microfilament assembly, FA maturation, and lamellipodia in migrating cells [31], while the different roles of two ROCK isoforms remained unclear. Currently, some evidence has indicated that ROCK1 and ROCK2 differentially participate in cell polarity generation in fibroblasts and the dendritic spine [32]. Whether these two isoforms differently mediate cancer cell motility and mechanotransduction has not yet been explored systematically.

In this study, we aimed to investigate the different functions of ROCK1 and

ACCEPTED MANUSCRIPT

ROCK2 in breast cancer cells in response to substrate stiffness. PAA gels with various elasticity moduli were elaborated to mimic the tissue stiffness of the normal breast tissue and the malignant and the bone metastasis stages of breast tumors [33, 34]. We hypothesized and verified that substrate stiffness could regulate cytoskeleton reorganization and traction force generation, thus promoting cell motility. We also systematically analyzed the different signaling cascades involving ROCK1 and ROCK2 response to substrate stiffness in MDA-MB-231 cells. Considered together, our study closely examined the relationship between substrate stiffness and tumor cellular functions including motility and mechanotransduction; elucidated the molecular mechanisms involved, for instance, RhoA/ROCK1/p-MLC and RhoA/ROCK2/p-cofilin signaling pathways; and provided new insights into the metastasis mechanism research and clinical treatment of breast cancer.

2. Materials and methods

2.1. Preparation of polyacrylamide (PAA) gel substrates

PAA gel substrates were prepared as described previously [15]. Briefly, a mixed solution containing 40% acrylamide and 2% bis-acrylamide in varying proportions, 10% ammonia persulfate (Bio-Rad), and 0.05% TEMED (Sigma) was prepared and added to a gel mold to yield a gel with a final thickness of 0.75 mm. After gel polymerization at room temperature, sulfosuccinimidyl-6-(4'- zido-2'-nitrophenylamino) hexanoate (Sulfo-SANPAH;

ACCEPTED MANUSCRIPT

Thermo Scientific) was used to activate the gel surface under UV light for 20 min. These gels were then coated with type I collagen (0.25 mg/ml) in phosphate-buffered saline (PBS) and incubated overnight at 4°C. On the subsequent day, the collagen solution was removed from the gels, which were then kept in PBS at 4°C until use.

2.2. Cell culture

The MDA-MB-231 human breast cancer cell line was obtained from the American Type Culture Collection (ATCC). Cells were cultured in L-15 culture medium supplemented with 10% newborn calf serum (Thermo Scientific) and 1% streptomycin and penicillin in a 37°C humidified incubator without CO_2 atmosphere. MCF-7 and MDA-MB-468 were grown in RPMI-1640 medium supplemented with 10% newborn calf serum and 1% streptomycin and penicillin and incubated at 37°C in 5% CO_2.

2.3. Antibodies and reagents

The following antibodies were used: β1 integrin and RhoA from Abcam (USA); FAK and phospho-FAK (p-FAK; Tyr397) from BD Transduction Laboratories™ (USA); phospho-Paxilin (p-Paxilin; Tyr118), phospho-myosin regulatory light chain (p-MRLC; Thr18/Ser19) and phospho-cofilin (p-cofilin; Ser3) from Cell Signaling Technology (USA); ROCK1, ROCK2, and MRLC from Proteintech (USA); and cofilin from Ruiying Biological (China). The TRITC-conjugated phalloidin was purchased from Sigma (USA). All of the

ACCEPTED MANUSCRIPT

other reagents were used as received without additional purification, unless otherwise noted.

2.4. Plasmids and transfection

Plasmids encoding pEGFP-COF-S3E (expresses pseudo-phosphorylated, nonactivatable cofilin fused to EGFP in mammalian cells) was obtained a gift from James Bamburg. pEGFP-MRLC1 T18D, S19D plasmid (expresses pseudo-phosphorylated, activatable MRLC fused to EGFP in mammalian cells), and pEGFP-MRLC1 were received as kind gifts from Prof. Thomas T Egelhoff (Cleveland Clinic, USA). Rock isoform-specific shRNA sequences were cloned into a pSGU6/GFP/Neo vector (Sangon, China), and the scrambled pSGU6/GFP/Neo vector was used as a control. The following sequences were used: ROCK1 shRNA, 5'-GCGCAATTGGTAGAAGAATGT-3'; ROCK2 shRNA, 5'-GGATATTCCAGATTCTGTATG-3'; and shNC, 5'-GTTCTCCGAACGTGTCACGT-3'. Cells were transfected with Lipofectamine® LTX (Invitrogen; USA) according to the manufacturer's protocol.

2.5. Western blot analysis

Cells lysed in RIPA Lysis Buffer (Beyotime, China) after being washed in cold PBS were separated by SDS-PAGE and transferred to PVDF membranes (Millipore, USA). The membranes were blocked with 5% nonfat dry milk (or 3% BSA for tyrosine phosphorylation blots) in TBST buffer (10 mM Tris-HCl, 100

ACCEPTED MANUSCRIPT

mM NaCl, and 0.1% Tween 20) for 1 h at room temperature before incubation with the following primary antibodies: β1-integrin (mouse mAb; 1:1000), RhoA (rabbit mAb; 1:1000), FAK (mouse mAb; 1:1000), p-FAK (mouse pAb; 1:1000), ROCK1 (rabbit pAb; 1:1000), ROCK2 (rabbit pAb; 1:500), MRLC (rabbit pAb; 1:1000), cofilin (rabbit pAb; 1:500), p-MRLC (rabbit mAb; 1:1000), p-cofilin (rabbit mAb; 1:1000), and β-actin (mouse mAb; 1:1000). After being washed to remove nonbound primary antibodies, the membranes were incubated with the corresponding secondary antibody at 1:2000-10,000 dilution at room temperature for 2 h. The membranes were washed three times with TBST, and immunoreactive signals were detected using the western blotting Luminol Reagent (Beyotime, China), according to the manufacturer's instructions.

2.6. Fluorescence staining and confocal microscopy

Cells were plated onto polyacrylamide gel substrates or glass coverslips and fixed in 4% paraformaldehyde for 15 min at room temperature. Then, they were permeabilized in 0.1% Triton X-100 for 10 min and blocked in 5% BSA for 1 h in 37°C. The cells were incubated with p-Paxilin (rabbit pAb; 1:50), ROCK1 (rabbit pAb; 1:50), and ROCK2 (rabbit pAb; 1:25) at 4°C overnight. Then, they were incubated with secondary antibodies coupled to Alexa Flour 488, Alexa Flour 594, or TRITC-labeled phalloidin for 1 h at 37°C. The samples were washed with PBS, and the cell nuclei were stained by DAPI. Fluorescence images were obtained using an inverted fluorescence microscope (Nikon

ACCEPTED MANUSCRIPT

TE-2000 and ZEIS LSM800).

2.7. Quantitative real-time RT-PCR (qRT-PCR)

RNA was extracted using TRIzol (Invitrogen, USA). cDNA was synthesized with the PrimeScript™ RT Reagent Kit (Takara, Japan). *q*PCR was performed with SYBR Premix Ex Taq™ II (Takara, Japan) using a CFX96™ Real-Time System (Bio-Rad, USA). The primer sequences were as follows: RhoA: 5′-CAGAAAAGTGGACCCCAGAA-3′ and 5′-GCAGCTGCTCTCGTAGCCATTTC-3′; ROCK1: 5′-AACATGCTGCT-GGATAAATCTGG-3′ and 5′-TGTATCACATC GTACCATGCCT-3′; ROCK2: 5′-ATGAAGGCAGAAGACTATGA-3′ and 5′-CTTGTGACGAACCAACTG-3′.

2.8. Traction force microscopy (TFM)

We used TFM to evaluate changes in cell contractility, as previously described [35]. In brief, to prepare gel substrates for cell traction measurements, a 0.01% suspension of 0.5-μm diameter red fluorescent beads (Invitrogen, USA) were added to the gel solution. After gel polymerization, the surface was functionalized as mentioned above. Cells were seeded and allowed to adhere and spread for two days. Phase-contrast images of the cell boundaries and the fluorescent beads at the surface of the gel were acquired. The cells were then removed by trypsinization, and another image of the bead positions was obtained (Nikon TE-2000U, Japan).

To analyze the total force exerted by a cell on the ECM, correlation-based

ACCEPTED MANUSCRIPT

particle image velocimetry (MATLAB, USA) was used to compute the image registration and track bead displacements. Displacements were then applied as a boundary condition on the surface of the gel, and the root mean square (RMS) traction stresses, net contractile moment, and maximum traction field on the gel surface were calculated using the COMSOL finite element package (COMSOL Multiphysics, USA) [31].

2.9. Atomic force microscope (AFM)

The elastic modulus of polyacrylamide gel substrates was determined by AFM (Agilent 5500, Agilent Technologies, USA). Measurements were performed in water in contact mode to prevent drying of the gels. A spherical-tipped indenter (with a radius of less than 10 nm) was used, and a force–displacement curve was obtained for the loading and unloading paths. The mechanical properties of the gels were determined for each separate experiment and averaged (mean ± SD) using three gels for each stiffness group.

For morphometric analysis, cells cultured on substrates of different stiffness were fixed in 4% paraformaldehyde and then observed. Deflection images revealed the cell membrane submicroscopic structures such as protrusions. Topographic images showed the heights of individual cells, and the profiles of cells were extracted from topographic images (white segment) using ImageJ software (USA). 3D reconstitution of topographic images was

ACCEPTED MANUSCRIPT

performed using Gwyddion. The number of filopodia, length of filopodia, lamellipodia surface area per cell, and number of lamellipodia each group were also quantified using ImageJ software [36].

2.10. Cell migration and invasion assay

To assess cell migration, cells were seeded at a density of 3×10^5 cells/mL in both chambers of an Ibidi-silicone insert (Ibidi, Germany). This insert allows for the formation of a well-defined “edge” without physically scratching or wounding the cell monolayer. Cells were cultured for 12 h to form a confluent monolayer before careful removal of the insert, and images were acquired after 24 h (Nikon Eclipse TE2000-U, Japan).

For the invasion assays, cells cultured on substrates of different stiffness for 48 h were removed by trypsinization and then seeded into the upper compartment (3×10^4 cells/well) of a transwell chamber (Corning, USA). After incubation for 12 h, cells that did not invade in the upper wells were removed with cotton swabs. Cells that had passed through the membrane on the lower surface of the insets were fixed with 4% paraformaldehyde and stained using crystal violet. These data were quantified using ImageJ software.

2.11. Time-lapse microscopy

The motility of MDA-MB-231 cells cultured in L-15 medium was performed by time-lapse microscopy. The locations of all cells were recorded and used to draw the track. ImageJ software was used to calculate the Euclidean distance

ACCEPTED MANUSCRIPT

(d_{Euclid}), average cell velocity (V), accumulated distance (d_{accum}), and directionality (D) of each group. It is to be noted that the persistence of cell motility in a preferred direction was assessed by computing a directionality for each cell, defined as $D= d_{Euclid}/d_{accum}$, while D=1 indicates that the cells moved along a straight line.

2.12. Fluorescence recovery after photobleaching (FRAP)

FRAP was performed using a confocal microscope (ZEIS LSM800). Cells were seeded at a low density in a 6-well plate for 24 h and transfected with GFP-MRLC, and experiments were performed 48 h later. After acquiring prebleach images, a small area within the actomyosin filament bundles in peripheral protrusion was bleached with the 488 line of the SIM scanner and recovered until the intensity reached a plateau and normalized to the prebleaching intensity [26].

2.13. Statistical analysis

Each experiment was performed at least three times. All the data are expressed as mean ± SD using GraphPad Prism software, version 6.0. Statistical analyses were performed with the t-test or one-way analysis of variance with post hoc multiple comparisons. The significant differences between groups were considered at a minimum value of $P<0.05$.

3. Results

ACCEPTED MANUSCRIPT

In this study, PAA hydrogel with controllable stiffness was used as the substrate and was coated with type I collagen on its surface for cell culture. The preparation method of PAA gel substrate is shown (Supplementary **Fig. S1A**). AFM is widely implemented to measure PAA gel stiffness. Consistent with the findings of previous reports, an increase in the cross-linking ratios of the acrylamide increased the stiffness of PAA gels [15]. Variations in elastic modulus with change in acrylamide concentration are presented as shown in Supplementary **Fig. S1B**. Briefly, PAA gels with elastic modulus values of 10 kPa, 38 kPa, and 57 kPa were denoted as soft, stiff, and rigid, respectively. These PAA gels were used to simulate the tissue stiffness at different progress stages of breast cancer *in vitro* [33, 34] and subsequently to investigate how substrate stiffness affects tumor cell motility and mechanical properties in breast cancer progression, which might provide a basis for studying the metastatic mechanisms and treatment of breast cancer.

3.1. Stiff substrate facilitates migration phenotype formation and cytoskeletal dynamics

The remarkable polygonal shapes of cells are widely considered as the morphology related to enhanced migration and invasion [4]. We first cultured MDA-MB-231 human breast cancer cells on PAA gels with varying stiffness for 48 h, showing that most cells cultured on stiff substrates were polygonal, and most cells cultured on glass substrates were elongated (Supplementary **Fig. S2A**). As shown in Supplementary **Fig. S2B-C**, the increase in substrate

ACCEPTED MANUSCRIPT

stiffness was positively related to the extension of cells by the determination of cell surface area and polarity index. Therefore, stiff substrates might facilitate the migration of breast cancer cells.

TME can influence cell morphology by regulating the assembly of the cytoskeleton. In addition, actin polymerization at the leading edge of migrating cells is a precondition for cell motility [37]. Therefore, we speculated whether substrate stiffness could alter cytoskeleton reorganization. For this purpose, GFP-MRLC was used to exhibit the dynamic assembly of the microfilament cytoskeleton. The results showed that, while seeding MDA-MB-231 cells in stiff substrates, the assembled rate of the stress fibers was significantly higher than that in other groups, and the distribution of the stress fibers was mainly located at the cell edge. In contrast, the stress fibers on traditional glass substrates were evenly distributed in the cell body (**Fig. 1A**), suggesting that stiff substrates promote cell movement, likely in a more directional way. We also used TRITC-labeled phalloidin to examine the distribution of stress fibers in MCF-7 and MDA-MB-468 breast cancer cells. It was found that there is more F-actin polymerization in cell membrane protrusions when they are cultured on stiff substrates (Supplementary **Fig. S2D**). In contrast, there were few actomyosin filament bundles in the cells cultured on other substrates. Furthermore, to monitor the dynamic behavior of individual microfilaments, fluorescence recovery after photobleaching (FRAP) experiments on GFP-MRLC in peripheral protrusion were implemented. Recovery of

ACCEPTED MANUSCRIPT

fluorescence after photobleaching of microfilaments was substantially fast in the cells from stiff substrates (**Fig. 1B**). Quantification of the fluorescent intensity confirmed that an increased mobile fraction was present in the cells cultured on stiff substrates compared with that in other groups (**Fig. 1C**). Collectively, the microfilament cytoskeleton was more stable in cells cultured on soft and rigid substrates, suggesting that stiff substrates can facilitate the assembly of stress fibers.

3.2. Stiff substrates enhance cell migration and invasion

Cancer cells are more capable of metastasis and invasion, which accelerate the occurrence and development of tumors to a certain degree. At the same time, cell motility can be controlled by the cytoskeleton [31]. As substrate stiffness regulates cell spreading and microfilament reorganization, we considered whether cell migration and invasion behavior were also changed by substrates of different elastic moduli. To investigate these changes, we measured the sheet edge advancement over a period of 12 h after barrier removal (**Fig. 2A**). On the stiff substrate, the cohesive monolayer almost closed the gap and migrated in a directional, sheet-like fashion. In contrast, cells on each of the other three substrates showed more irregular movements than a random orientation (**Fig. 2B**). A similar phenomenon was observed in MDA-MB-468 cells (Supplementary **Fig. S3A** and **B**). Next, we used crystal violet staining to detect the cell invasion ability. Compared to cells cultured on

ACCEPTED MANUSCRIPT

other substrates, cells cultured on the stiff substrate were more aggressive, with more cells invading the outer sides of the inserts (**Fig. 2C** and **D**).

To assess the role of substrate stiffness in single-cell motility, time-lapse microscopy was performed to analyze individual cell movements cultured on different substrates. To quantify these differences in cell migration, individual cells were tracked for 4 h, and representative tracks for 50 cells on each substrate were exhibited (**Fig. 2E** and **F**). Subsequently, we presented a measurable analysis of these cell migration patterns to characterize the migratory properties (**Fig. 2G-J**). It is worth noting that cells seeded on soft substrates seemed to search for a suitable adherent site with little movement, and their behaviors represented a poor cell–matrix interaction. Particularly, cells growth on stiff substrates showed significantly fast migration velocity and longer distance, including accumulated distance and Euclidean distance. Moreover, there was no significant difference in the directionality for cells on stiff and rigid substrates. Therefore, it was clear that cells on soft and rigid substrates had poor migration and invasion ability, which was not conducive to the reconstruction of the cytoskeleton. These findings suggested that the stiff substrate favored cell reshaping, thus mediating cell motility in a fast and highly directional pattern, both in single-cell migration and in collective migration.

3.3. Stiff substrates promote the formation of leading-edge protrusion by FA maturation through polarizing traction force distribution

ACCEPTED MANUSCRIPT

The leading-edge protrusions on the cytomembrane are known to guide cell motility. During collective migration, cells at the leading edge and within the cell sheet all energetically migrate, the latter with the assistance of lamellipodia protrusions extending beneath adjacent cells [38]. In particular, filopodia formation is considered to be critical for cell invasion [5]. We therefore assessed membrane protrusion by atomic force microscopy (AFM), which was performed to reveal the cell membrane submicroscopic structures. Our results indicated that a stiff substrate was able to promote the formation of the migratory phenotype, in which the cells were polygonal and typically contained a large broad lamellipodium with numerous longer filopodia. In addition, it was observed that the cell height in the control group was 1 μm smaller than that in the other groups, which ranged from 2-3 μm (**Fig. 3A**). Quantitative statistical analyses are shown in **Fig. 3B-E**. Similar results were detected by time-lapse microscopy, with the cells grown on stiff substrates showing markedly increased motility as the morphology quickly changed, forming the typical fan-shaped lamellipodium in the front edge of migrating cells, while cells grown on soft substrates displayed fewer filopodia and smaller lamellipodia than those in other groups (Supplementary **Fig. S3C**). Thus, the present data revealed that stiff substrates contributed to the formation and extension of leading edge protrusions and would in turn regulate cell motility.

The formation of membrane protrusions at the leading cell edge is dependent on the formation and maturation of FA [26]. To better understand

ACCEPTED MANUSCRIPT

how cell motility was altered by substrate stiffness, MDA-MB-231 cells were immunostained for F-actin and p-paxillin to examine the FA dynamics. Particularly, the formation and turnover of FAs play important roles in regulating cell migration, and tyrosine phosphorylation of paxillin has been implicated in the assembly of FAs [39]. We therefore hypothesized that the increased cell motility observed with stiff substrates might be due to substrate stiffness-dependent phosphorylation of paxillin in membrane protrusions. As shown in **Fig. 4A**, cells cultured on stiff substrates for 48 h developed numerous, larger, more mature FAs, closely associated with actin bundles in the lamellipodia and the cell bodies. In contrast, we noted that other groups only exhibited a dot-like staining pattern concentrated near the cell periphery. Quantitatively, cells grown on stiff substrates underwent a 2-fold increase in total FAs and a 4-fold increase in mature FAs (larger than 1 μm^2) than the control group (**Fig. 4B**). Overall, we concluded that substrate stiffness-dependent formation and maturation of FAs lead to enhanced cell motility.

FA maturation is dependent on the traction forces generated by nonmuscle myosin II (NM II). For typical migration cells, cell-induced traction forces are exerted on the underlying substrate, as cells attach to form new adhesions at the leading edge and detach to disassemble adhesions at the rear of the cells [22]. To further investigate how substrate stiffness alters the traction stress generated by MDA-MB-231 cells, TFM was used as illustrated

ACCEPTED MANUSCRIPT

earlier (Supplementary **Fig. S1C**). The data showed that the average force in cells increased with the increase in extracellular substrate stiffness, and the maximum traction was mainly distributed at the rear of the cells (**Fig. 4C**). The traction forces exerted by round cells seeded on soft substrates were significantly lower than that in the other groups, as well as the net contractile and maximum traction. Interestingly, there was no significant difference in the degree of cell contraction on stiff and rigid substrates, and both were higher than those on soft substrate, which could reflect the displacement of embedded fluorescent beads (**Fig. 4D-G**). This finding indicated that the degree of cell deformation was similar on stiff and rigid substrates, but the traction force of cells on rigid substrate was higher than that on stiff substrate due to the change in ECM stiffness. Moreover, previous studies have demonstrated that there is a positive correlation between ECM stiffness and tumor cell stiffness, and the extreme increase in cellular stiffness weakens the ability of cytoskeleton to undergo dynamic state changes [10, 12], therefore compromising tumor cell motility on an excessively rigid substrate.

3.4. RhoA, ROCK1, and ROCK2 signaling enhances cell motility in a substrate stiffness-dependent manner through integrin β1

During tumorigenesis, gene expressions are always altered. RhoA, an important small GTPase, is a key factor in cell migration and invasion in breast cancer [40]. The above results indicated that substrate stiffness was able to

ACCEPTED MANUSCRIPT

mediate cell motility; hence, we attempted to investigate whether the RhoA/ROCK signaling pathway was involved in the regulation of this process. Consequently, RhoA, ROCK1, and ROCK2 mRNA and protein levels were analyzed in cells exposed to various degrees of ECM stiffness. Quantitative real-time RT-PCR (*q*PCR) revealed that RhoA, ROCK1, and ROCK2 mRNA levels increased in cells cultured on stiff substrates (Supplementary **Fig. S4A-C**). In agreement with the *q*PCR results, western blot showed that RhoA, ROCK1, and ROCK2 protein levels also increased modestly after 48 h on a stiff substrate and were associated with MRLC phosphorylation at Thr18/Ser19, which was the key molecule that mediated the activity of NM II. However, the enhancement of phosphorylation levels in the actin-severing protein cofilin was not significant on stiff substrates (**Fig. 5A**).

To determine the clinical relevance of RhoA, ROCK1, and ROCK2 overexpression in human breast cancer, survival data were analyzed by stratifying patients according to these mRNA levels in the primary tumor (Supplementary **Fig. S4D-F**). We observed that higher levels of RhoA, ROCK1, and ROCK2 mRNA were strongly correlated with decreased patient survival, potentially implicating RhoA, ROCK1, and ROCK2 signaling in breast cancer progression. Considered together, the data presented above showed that RhoA, ROCK1, and ROCK2 signaling was positively connected to breast tumor cell motility in a substrate stiffness-dependent manner.

Integrins are transmembrane receptors that link cells and the ECM. In

ACCEPTED MANUSCRIPT

signal transduction, integrins transmit signals into cells related to the chemical composition and mechanical state of TME, participating in multiple cell functions such as cell survival, proliferation, apoptosis, and migration [17]. In addition, cell growth on many substrates depends on integrin-mediated cytoskeletal and signal transduction molecules such as FAK [41]. We questioned whether integrin β1-mediated signaling was required for cell motility in a substrate stiffness-dependent manner. Therefore, we explored the integrin β1 and FAK expression in MDA-MB-231 cells (**Fig. 5A**). Consistent with our assumptions, western blot analysis elucidated that integrin β1 and pFAK levels were high in cells cultured on stiff substrates. Moreover, immunofluorescence images indicated that cells cultured on stiff substrates demonstrated a significant increase in the activation of integrin β1, accompanied by apparent internalization (**Fig. 5C** and **D**). Generally, the internalization of integrin contributes to the maturation and turnover of FAs [20]. Furthermore, cells seeded on substrates of different stiffness pretreated with anti-integrin β1 antibodies for 6 h showed no significant variations in the phosphorylation levels of FAK, MRLC, and cofilin (**Fig. 5B**), confirming that substrate stiffness-induced cell motility is mediated by the expression and activation of integrin β1.

3.5. ROCK1 and ROCK2 localize to specific cytoskeletal assemblies

ROCK, as one of the Rho effector proteins, has been considered to play

ACCEPTED MANUSCRIPT

an important role in RhoA-mediated stress fiber formation and FA composition [30]. We sought to determine the different effects of ROCK1 and ROCK2 on cytoskeletal organization. For this aim, immunofluorescence staining was used to investigate the distribution of these two ROCK isoforms. Surprisingly, our results showed that ROCK1 and ROCK2 showed specific localization patterns in cells. The white regions of the cells were ROCK1 or ROCK2 colocalized with F-actin (**Fig.6A**). ROCK1 was strongly distributed in actin bundles along the dorsal side of cells, while ROCK2 was located at the edge of cell membrane protrusions. Given the essential role of substrate stiffness in cell motility, we further analyzed the influence of ECM stiffness on the distribution of ROCK1 and ROCK2. Quantification data exhibited that there are more ROCK1 and ROCK2 localized to actomyosin filament bundles and membrane protrusions in cells cultured on stiff substrate, respectively (**Fig.6B** and **C**). Together, these results lead us to hypothesize that substrate stiffness may distinctively regulate these two ROCK isoforms in cytoskeletal assemblies and then regulate tumor cell motility.

3.6. ROCK1 and ROCK2 differentially phosphorylate MRLC and cofilin

To evaluate whether substrate stiffness-mediated ROCK1 and ROCK2 differentially regulated cytoskeletal assemblies, we constructed ROCK isoform-specific shRNAs to examine the phosphorylation of ROCK downstream targets, for instance, MRLC and cofilin [32]. MDA-MB-231 cells

ACCEPTED MANUSCRIPT

were cultured on stiff substrates for 24 h and then transfected with ROCK isoform-specific shRNAs. After 48 h, the expression of ROCK1 and ROCK2, MRLC phosphorylation, and cofilin was determined by western blotting (**Fig. 7A-C**). Notably, knockdown of ROCK1, but not ROCK2, specifically reduced MRLC phosphorylation, whereas the silencing of ROCK2 resulted in decreased p-cofilin. Thus, ROCK1 altered myosin II activity through regulatory light chain Thr18/Ser19 phosphorylation, and ROCK2 regulated actin polymerization through cofilin Ser3 phosphorylation, which could combine to generate stable actomyosin filament bundles driving the formation and maturation of FAs.

We then assessed the impact of knockdown of ROCK1 or ROCK2 on cell morphology, including cell surface area and polarity index (**Fig. 7D**). Our results indicated that MDA-MB-231 cells with ROCK1 knockdown failed to polarize, as well as the significant decrease in surface area compared with controls. However, ROCK2-knockdown cells were elongated with an increased polarity index, but there was no remarkable influence on surface area (**Fig. 7E** and **F**). To confirm the above results, MRLC-DD and COF-S3E phosphomimetic mutants were used to rescue the observed knockdown phenotypes. Indeed, as we transfected these two mutants into cells with specific ROCK isoform knockdown, the cell morphological parameters were restored to the level of the control group. We also found that cell polarity was enhanced when MRLC-DD was transferred into cells alone. Nevertheless,

ACCEPTED MANUSCRIPT

after COF-S3E was transferred, cell polarity and area decreased significantly (Supplementary **Fig. S5A-C**). Collectively, the differential phosphoregulation of MRLC and cofilin by ROCK1 and ROCK2 contributed to the formation of cell morphology.

3.7. ROCK1- and ROCK2-induced MRLC and cofilin phosphorylation promotes cell directional migration by facilitating cytoskeleton organization and FA maturation

Cell morphology is important to numerous cell behaviors and functions [3, 42]. Thus, we evaluated the effects of MRLC and cofilin phosphorylation on the migration of breast cancer cells and analyzed these cell migration patterns to characterize the migratory properties by time-lapse video microscopy, combined with individual cell tracking [43]. Interestingly, ROCK1 and ROCK2 downregulation in MDA-MB-231 cells by shRNA decreased track length and the directionality of migration compared with that in control cells (**Fig. 8A** and **B**). The data supported the idea that ROCK presence in these cells favored the persistence of cell motility. Indeed, both ROCK isoform knockdown decreased cell migration-associated parameters, including instant velocity, Euclidean distance, and directionality, but there was no significant effect on accumulated distance (**Fig. 8C-F**). However, the co-expression of MRLC-DD or COF-S3E rescued cell directional migration. These results suggested that MRLC and cofilin phosphorylation were necessary for the regulation of cell motility.

We next explored the effects of MRLC and cofilin phosphorylation on FA

ACCEPTED MANUSCRIPT

maturation and cytoskeleton structure formation. Both ROCK isoform knockdown resulted in significantly smaller FAs and a lack of stress fibers than that in control cells (Supplementary **Fig. S5D-F**). To better observe the density and thickness of stress fibers, we drew a line profile across the cytoplasm to analyze the cytoskeleton structure formation. Our results indicated that, regardless of which ROCK isoform-specific shRNA was transferred, it was not conducive to F-actin organization, with a dot-like depolymerized form instead of distinct and sharp peaks on fluorescence intensity graphs. In comparison, the co-expression of MRLC-DD or COF-S3E rescued stress fiber formation, with which F-actin was assembled to form thick fibers abundantly localized throughout the cytoplasm (Supplementary **Fig. S5D**).

Furthermore, a clear difference was also observed in FA maturation by immunofluorescence staining. Of interest, cells depleted of ROCK1 or ROCK2 exhibited small, nascent FAs that failed to enlarge, demonstrating that FA maturation was stabilized by stress fibers, perhaps because the silence of each ROCK isoform is able to disrupt actomyosin filament contraction and bundling. Analysis of FA number per cell showed that the decrease in MRLC and cofilin phosphorylation levels mainly reduced FA size, significantly influencing the number of larger, mature FAs in membrane protrusions (Supplementary **Fig. S5F**). Similar to effects of these mutants on cytoskeletal dynamics, stabilization of mature FAs at the cell edge could be rescued by co-expressing MRLC-DD or COF-S3E in ROCK isoform-deficient cells.

ACCEPTED MANUSCRIPT

Accordingly, the MRLC- and cofilin-mediated microfilament contracting and remodeling regulated FA maturation and cytoskeleton structure formation.

3.8. ROCK1- and ROCK2-induced MRLC and cofilin phosphorylation mediates traction force generation and distribution

In addition to FA formation and actin filament network reconstruction, the generation of intracellular stress also plays a key role in cell polarization and migration [36]. To elucidate the correlation between ROCK isoform depletion and traction forces, TFM was used to detect the magnitude and distribution of cell traction forces. As cell morphology changes, so does the distribution of traction forces (**Fig. 9A**). The knockdown of both ROCK isoforms prevented the maximum traction distributed at the rear of the cells compared to the control group, thereby resulting in uncertain directionality. Notably, the displacement of fluorescence microbeads, used to indicate the deformation of substrate caused by intracellular stress, was apparently decreased in cells depleted of specific ROCK isoforms compared to the control group, with ROCK2 knockdown exhibiting RMS traction intermediate between the control and ROCK1 knockdown cells (**Fig. 9B** and **C**). Consistently, we also determined this tendency by calculating the net contractile moment and maximum traction, suggesting that ROCK1 dominates the regulation of traction forces. As NM II was directly downstream of ROCK1, it had certain advantages in the generation and distribution of cell traction forces compared with ROCK2 (**Fig. 9D** and **E**), while co-expressing MRLC-DD or COF-S3E in corresponding

ACCEPTED MANUSCRIPT

ROCK isoform-deficient cells could recover traction forces successfully.

4. Discussion

A growing body of evidence has indicated that physical properties of ECM affect and even control cell behaviors and functions, in which substrate stiffness, porosity, insolubility, spatial arrangement, and orientation (topological structure) play roles. Collectively, these properties determine the functional characteristics that maintain the integrity of tissue structure and directly regulate cell behaviors and mechanotransduction [14]. The production, cross-linking, degradation, and reconstruction of ECM components are dynamic processes, and abnormal ECM metabolism is often accompanied by the occurrence of diseases such as organization fibrosis and cancer [3]. During tumor development, the abnormal cross-linking and deposition of ECM result in continuous increase in substrate stiffness and further affect tumor cell behaviors including morphogenesis, proliferation, differentiation, apoptosis, and motility [44, 45]. Therefore, the use of imageology to detect tissue density or stiffness is of great clinical significance for the early detection and diagnosis of tumors [46], whereas the impact of substrate stiffness on breast cancer cells has been rarely reported, as well as the molecular mechanisms involved. Accordingly, the present study investigated the changes in MDA-MB-231 cell motility and mechanical behaviors in response to various degrees of substrate stiffness and assessed the underlying mechanotransduction pathways.

ACCEPTED MANUSCRIPT

Recently, some discoveries have shown that an implanted scaffold could identify and recruit metastatic cancer cells in vivo, thus also effectively decreasing the emergence of metastatic lesions in other organs such as the lung, liver, and brain [47, 48]. The present work showed that low ECM stiffness can reduce cell motility, which might provide new enlightenment regarding the determination of scaffold stiffness.

4.1. Substrate stiffness-dependent phenotype formation and integrin β1-activated FAK in malignant tumor cells

Here, PAA gels were adopted as an *in vitro* matrix model with which we could deliberately tune the substrate stiffness to investigate the mechanical interactions between human breast cancer cells and substrates. For determining the stiffness of substrates, we used PAA gels with a Young's modulus of 10 kPa to mimic normal breast tissue and benign breast tumors and 38 kPa to mimic malignant breast tumors [33]. However, the tumor tissue stiffness could reach a Young's modulus of 50-60 kPa after bone metastasis; thus, 57 kPa was used to simulate the advanced stages of breast tumors that are more rigid than any breast tissue and close to bone stiffness [34]. We found that MDA-MB-231 cells cultured on substrates of different stiffness displayed various cell morphologies and cytoskeletal organizations. Interestingly, high matrix stiffness could induce the emergence of a malignant phenotype, with high capacity for migration and invasion.

ACCEPTED MANUSCRIPT

It is well established that cell adhesion and morphology can influence the subsequent behaviors of cells [26, 41]. Cell adhesion is the first stage of cell–substrate interactions and will affect the subsequent cell motility and mechanical behaviors. In the response of cells to substrate stiffness, integrin-β1 in FA-mediated mechanotransduction is an “outside–in and inside–out” mechanism, and this signaling loop is essential for cell behavior and functions as a signaling center orchestrating a network of signaling pathways [20, 49]. When cells were cultured on stiff substrates, integrin β1 was activated, thus upregulating FAK phosphorylation, which was required for cell adhesion and migration. Numerous studies have reported that cell migration is a highly complex, multistep process initiated through FA formation and maturation, followed by membrane protrusion emergence, including filopodia, lamellipodia, and invadopodia, which are tightly coupled with the dynamics of both actin assembly and actin disassembly [37, 50]. The traction force produced by actin–myosin contractility is used to detach cells near FAs from the ECM, while ECM stiffness can promote the formation of FAs [51].

4.2. The dual effect of substrate stiffness on cell motility

In this study, we noticed that cells cultured on stiff substrates exhibited higher migration and invasion abilities than those in other groups, with more mature FAs, filopodia, and larger lamellipodia at the leading edge of migrating cells. Consistent with the findings of previous studies, only in a certain range,

ACCEPTED MANUSCRIPT

increasing substrate stiffness is conducive to cell spreading and stress fiber reconstruction, thus promoting cell motility [42, 52], mainly because the increase in ECM stiffness is positively correlated with cell stiffness, while excessive cell stiffness is not benefited to cell deformation and movement, making tumor cells less likely to pass through the dense ECM smoothly in the process of metastasis [53, 54]. Conversely, growing evidence has found that tumor cells with greater migration and metastasis ability are more flexible [55, 56]. In addition, studies have shown that the influence of substrate stiffness on tumor cell proliferation is related to the targeting of organ metastases in cell subtypes. Research on different subtypes of the MDA-MB-231 human breast cancer cell line from a single cell source has observed that the proliferation of each subtype is strongest on a substrate with stiffness similar to that of its preferred metastatic target organ [57]. These findings suggest that tumor cells are a heterogeneous population in which subtypes with diverse characteristics respond differently to matrix mechanics.

4.3. The differential regulatory mechanism between two ROCK isoforms in cell motility and mechanotransduction

Overexpression of RhoA is a common event in breast cancer that promotes tumor cell proliferation and metastasis [40]. In typical migrating cells, active Rho binds to ROCK, mediating the formation of actin stress fibers [58], with the generation of the contractile force required for cell tail retraction and

ACCEPTED MANUSCRIPT

FA turnover [38]. Here, we observed that the expression of RhoA, ROCK1, and ROCK2 was upregulated in MDA-MB-231 cells cultured on stiff substrates, further promoting the activation of downstream molecules-MRLC and cofilin and suggesting that the regulation of breast cancer cell motility mediated by substrate stiffness was dependent on the RhoA/ROCK signaling pathway.

Moreover, our study investigated the functional differences between the two isoforms of ROCK (ROCK1 and ROCK2) thoroughly with this model. As the two ROCK isoforms share a highly conserved kinase domain, it has been postulated that they might perform similar biological functions by phosphorylating common substrates [30]. Indeed, previous studies explored how ROCK impacts the biological behavior of breast cancer cells in generalities [31, 59]. However, there have been various reports suggesting that ROCK proteins exhibit distinct functions and regulation. In the formation of epithelial zonula adherens (ZA), ROCK1, but not ROCK2, was necessary to stabilize GTP-RhoA at the ZA, thereby sustaining junctional tension through nonmuscle myosin IIA and inhibiting intraepithelial cell movement [60]. For cell–matrix adhesion, ROCK1 was essential for the maturation of FA complexes and cytoskeletal reconstruction, while ROCK2 deficiency increased the generation of stress fibers and FAs [61, 62]. Using ROCK isoform-specific shRNAs, we found that only knockdown of ROCK1 significantly decreased the level of p-MRLC, and ROCK2 played a critical role in the activation of cofilin. Furthermore, the deficiency of either ROCK1 or ROCK2 remarkably reduced

ACCEPTED MANUSCRIPT

cell motility, and it was not conducive to cytoskeleton remodeling, FA maturation, and contractility generation as well. Hence, it could be assumed that the two ROCK isoforms distinctively regulate the activation of downstream signaling molecules. Consistent with the findings of previous studies, the transfection of phosphomimetic mutants at specific sites has been shown to restore the migratory behavior [32]. In addition, it was noteworthy that the differences in the distribution of ROCK1 and ROCK2 in cells also indicate differences in their functions. These results shed insight into the molecular mechanisms of substrate stiffness-induced cell motility.

5. Conclusion

In summary, stiffness-regulatable polyacrylamide substrates were used to mimic tissue stiffness *in vitro* at different breast cancer stages. We found that moderate substrate stiffness promoted breast cancer cell motility through integrin β1-FAK-mediated mechanotransduction pathways. Stiff substrates, rather than soft, rigid, or traditional glass substrates, induce the emergence of malignant phenotypes. Subcellular structure observation showed that stiff substrates promote the formation of leading-edge protrusion by accelerating focal adhesion maturation and polarizing intracellular traction force distribution. Moreover, the expression of RhoA, ROCK1, and ROCK2 was upregulated following FAK activation. The different regulatory roles between the two ROCK isoforms in cell motility were extensively explored. It was found that ROCK1

ACCEPTED MANUSCRIPT

phosphorylated the myosin-regulatory light chain and facilitated the generation of traction force, while ROCK2 phosphorylated cofilin and regulated cytoskeletal remodeling by suppressing F-actin depolymerization in a substrate stiffness-dependent manner. The mechanotransduction model is summarized in **Fig. 10**, in which substrate stiffness activates integrin β1, hence transforming mechanical signals into biochemical signals. Then, these signals mediate the RhoA/ROCK1/p-MLC and RhoA/ROCK2/p-cofilin pathways through FAK activation and eventually augment cell motility. Our research revealed that substrate stiffness has profound influences on the migratory and malignant behaviors of human breast cancer cells, including morphology transformation, cytoskeletal rearrangement, lamellipodia formation, focal adhesion maturation, and traction force generation, consequently regulating cell motility. Most importantly, ROCK isoform-specific functions of cell traction force generation and cytoskeletal remodeling were distinguished, which could have significant implications in the understanding of the interaction between cancer cells and tumor microenvironments. Taming these physical forces by implanting scaffolds with specific stiffness or by inhibiting specific ROCK isoforms could have potential implications for improving therapeutic outcomes in cancer.

Acknowledgments

This work was supported by the National Natural Science Foundation of

ACCEPTED MANUSCRIPT

China (11772088, 31470906, 11502049, 31700811, 11802056, 31800780, 81471785, 31470959, and 81671821), the China Postdoctoral Science Foundation (2016M592657, 2017JY0217, and 2018M640904), the Basic Research Program of Sichuan Science and Technology Foundation (2017JY0019 and 2017JY0217), and the Fundamental Research Funds for the Central Universities (ZYGX2016Z001 and ZYGX2017KYQD180).

Data availability. The data sets generated during and/or analyzed during the current study are available from the corresponding author on reasonable request.

References

[1] R.L. Siegel, K.D. Miller, A. Jemal, Cancer Statistics, 2017, CA Cancer J Clin 67(1) (2017) 7-30.

[2] J.D. Humphrey, E.R. Dufresne, M.A. Schwartz, Mechanotransduction and extracellular matrix homeostasis, Nat Rev Mol Cell Biol 15(12) (2014) 802-12.

[3] L. Kass, J.T. Erler, M. Dembo, V.M. Weaver, Mammary epithelial cell: influence of extracellular matrix composition and organization during development and tumorigenesis, Int J Biochem Cell Biol 39(11) (2007) 1987-94.

[4] C.M. Kraning-Rush, C.A. Reinhart-King, Controlling matrix stiffness and topography for the study of tumor cell migration, Cell Adh Migr 6(3) (2012) 274-9.

[5] F. Zhao, L. Li, L. Guan, H. Yang, C. Wu, Y. Liu, Roles for GP IIb/IIIa and alphavbeta3

ACCEPTED MANUSCRIPT

integrins in MDA-MB-231 cell invasion and shear flow-induced cancer cell mechanotransduction, Cancer Lett 344(1) (2014) 62-73.

[6] H. Yang, L. Guan, S. Li, Y. Jiang, N. Xiong, L. Li, C. Wu, H. Zeng, Y. Liu, Mechanosensitive caveolin-1 activation-induced PI3K/Akt/mTOR signaling pathway promotes breast cancer motility, invadopodia formation and metastasis in vivo, Oncotarget 7(13) (2016) 16227-47.

[7] S. Li, Y. Chen, Y. Zhang, X. Jiang, Y. Jiang, X. Qin, H. Yang, C. Wu, Y. Liu, Shear stress promotes anoikis resistance of cancer cells via caveolin-1-dependent extrinsic and intrinsic apoptotic pathways, J Cell Physiol 234(4) (2019) 3730-3743.

[8] Y. Gu, Y. Ji, Y. Zhao, Y. Liu, F. Ding, X. Gu, Y. Yang, The influence of substrate stiffness on the behavior and functions of Schwann cells in culture, Biomaterials 33(28) (2012) 6672-81.

[9] S. Molladavoodi, H.J. Kwon, J. Medley, M. Gorbet, Human corneal epithelial cell response to substrate stiffness, Acta Biomater 11 (2015) 324-32.

[10] V.C. Shukla, N. Higuita-Castro, P. Nana-Sinkam, S.N. Ghadiali, Substrate stiffness modulates lung cancer cell migration but not epithelial to mesenchymal transition, J Biomed Mater Res A 104(5) (2016) 1182-93.

[11] F. Grinnell, C.H. Ho, The effect of growth factor environment on fibroblast morphological response to substrate stiffness, Biomaterials 34(4) (2013) 965-74.

[12] C. Chen, J. Xie, L. Deng, L. Yang, Substrate stiffness together with soluble factors affects chondrocyte mechanoresponses, ACS Appl Mater Interfaces 6(18) (2014) 16106-16.

[13] P.P. Provenzano, D.R. Inman, K.W. Eliceiri, J.G. Knittel, L. Yan, C.T. Rueden, J.G. White, P.J. Keely, Collagen density promotes mammary tumor initiation and progression, BMC Med 6 (2008) 11.

ACCEPTED MANUSCRIPT

[14] J.I. Lopez, I. Kang, W.K. You, D.M. McDonald, V.M. Weaver, In situ force mapping of mammary gland transformation, Integr Biol (Camb) 3(9) (2011) 910-21.

[15] J.R. Tse, A.J. Engler, Preparation of hydrogel substrates with tunable mechanical properties, Curr Protoc Cell Biol Chapter 10 (2010) Unit 10 16.

[16] F. Rehfeldt, A.J. Engler, A. Eckhardt, F. Ahmed, D.E. Discher, Cell responses to the mechanochemical microenvironment--implications for regenerative medicine and drug delivery, Adv Drug Deliv Rev 59(13) (2007) 1329-39.

[17] I.D. Campbell, M.J. Humphries, Integrin structure, activation, and interactions, Cold Spring Harb Perspect Biol 3(3) (2011).

[18] S.F. Badylak, Regenerative medicine and developmental biology: the role of the extracellular matrix, Anat Rec B New Anat 287(1) (2005) 36-41.

[19] T. Fischer, N. Wilharm, A. Hayn, C.T. Mierke, Matrix and cellular mechanical properties are the driving factors for facilitating human cancer cell motility into 3D engineered matrices, Convergent Science Physical Oncology 3(4) (2017) 044003.

[20] S. Li, N. Xiong, Y. Peng, K. Tang, H. Bai, X. Lv, Y. Jiang, X. Qin, H. Yang, C. Wu, P. Zhou, Y. Liu, Acidic pHe regulates cytoskeletal dynamics through conformational integrin beta1 activation and promotes membrane protrusion, Biochim Biophys Acta Mol Basis Dis 1864(7) (2018) 2395-2408.

[21] C. Zhang, H.J. Wang, Q.C. Bao, L. Wang, T.K. Guo, W.L. Chen, L.L. Xu, H.S. Zhou, J.L. Bian, Y.R. Yang, H.P. Sun, X.L. Xu, Q.D. You, NRF2 promotes breast cancer cell proliferation and metastasis by increasing RhoA/ROCK pathway signal transduction, Oncotarget 7(45) (2016) 73593-73606.

ACCEPTED MANUSCRIPT

[22] M. Parri, P. Chiarugi, Rac and Rho GTPases in cancer cell motility control, Cell Commun Signal 8 (2010) 23.

[23] X. Qin, B.O. Park, J. Liu, B. Chen, V. Choesmel-Cadamuro, K. Belguise, W.D. Heo, X. Wang, Cell-matrix adhesion and cell-cell adhesion differentially control basal myosin oscillation and Drosophila egg chamber elongation, Nat Commun 8 (2017) 14708.

[24] X. Qin, E. Hannezo, T. Mangeat, C. Liu, P. Majumder, J. Liu, V. Choesmel-Cadamuro, J.A. McDonald, Y. Liu, B. Yi, X. Wang, A biochemical network controlling basal myosin oscillation, Nat Commun 9(1) (2018) 1210.

[25] K. Ohashi, Roles of cofilin in development and its mechanisms of regulation, Dev Growth Differ 57(4) (2015) 275-90.

[26] N. Xiong, S. Li, K. Tang, H. Bai, Y. Peng, H. Yang, C. Wu, Y. Liu, Involvement of caveolin-1 in low shear stress-induced breast cancer cell motility and adhesion: Roles of FAK/Src and ROCK/p-MLC pathways, Biochim Biophys Acta Mol Cell Res 1864(1) (2017) 12-22.

[27] C.T. Mierke, T. Fischer, S. Puder, T. Kunschmann, B. Soetje, W.H. Ziegler, Focal adhesion kinase activity is required for actomyosin contractility-based invasion of cells into dense 3D matrices, Sci Rep 7 (2017) 42780.

[28] M.D. Schaller, Cellular functions of FAK kinases: insight into molecular mechanisms and novel functions, J Cell Sci 123(Pt 7) (2010) 1007-13.

[29] M. Luo, H. Fan, T. Nagy, H. Wei, C. Wang, S. Liu, M.S. Wicha, J.L. Guan, Mammary epithelial-specific ablation of the focal adhesion kinase suppresses mammary tumorigenesis by affecting mammary cancer stem/progenitor cells, Cancer Res 69(2) (2009) 466-74.

ACCEPTED MANUSCRIPT

[30] L. Julian, M.F. Olson, Rho-associated coiled-coil containing kinases (ROCK): structure, regulation, and functions, Small GTPases 5 (2014) e29846.

[31] I. Aifuwa, A. Giri, N. Longe, S.H. Lee, S.S. An, D. Wirtz, Senescent stromal cells induce cancer cell migration via inhibition of RhoA/ROCK/myosin-based cell contractility, Oncotarget 6(31) (2015) 30516-31.

[32] K.A. Newell-Litwa, M. Badoual, H. Asmussen, H. Patel, L. Whitmore, A.R. Horwitz, ROCK1 and 2 differentially regulate actomyosin organization to drive cell and synaptic polarity, J Cell Biol 210(2) (2015) 225-42.

[33] M. Plodinec, M. Loparic, C.A. Monnier, E.C. Obermann, R. Zanetti-Dallenbach, P. Oertle, J.T. Hyotyla, U. Aebi, M. Bentires-Alj, R.Y. Lim, C.A. Schoenenberger, The nanomechanical signature of breast cancer, Nat Nanotechnol 7(11) (2012) 757-65.

[34] E. Jabbari, S.K. Sarvestani, L. Daneshian, S. Moeinzadeh, Optimum 3D Matrix Stiffness for Maintenance of Cancer Stem Cells Is Dependent on Tissue Origin of Cancer Cells, PLoS One 10(7) (2015) e0132377.

[35] R. Zielinski, C. Mihai, D. Kniss, S.N. Ghadiali, Finite element analysis of traction force microscopy: influence of cell mechanics, adhesion, and morphology, J Biomech Eng 135(7) (2013) 71009.

[36] L.I. Volakis, R. Li, W.E.t. Ackerman, C. Mihai, M. Bechel, T.L. Summerfield, C.S. Ahn, H.M. Powell, R. Zielinski, T.J. Rosol, S.N. Ghadiali, D.A. Kniss, Loss of myoferlin redirects breast cancer cell motility towards collective migration, PLoS One 9(2) (2014) e86110.

[37] L.P. Cramer, Role of actin-filament disassembly in lamellipodium protrusion in motile cells revealed using the drug jasplakinolide, Curr Biol 9(19) (1999) 1095-105.

ACCEPTED MANUSCRIPT

[38] M.R. Ng, A. Besser, G. Danuser, J.S. Brugge, Substrate stiffness regulates cadherin-dependent collective migration through myosin-II contractility, J Cell Biol 199(3) (2012) 545-63.

[39] A.M. Pasapera, S.V. Plotnikov, R.S. Fischer, L.B. Case, T.T. Egelhoff, C.M. Waterman, Rac1-dependent phosphorylation and focal adhesion recruitment of myosin IIA regulates migration and mechanosensing, Curr Biol 25(2) (2015) 175-186.

[40] M. Caceres, J. Guerrero, J. Martinez, Overexpression of RhoA-GTP induces activation of the Epidermal Growth Factor Receptor, dephosphorylation of focal adhesion kinase and increased motility in breast cancer cells, Exp Cell Res 309(1) (2005) 229-38.

[41] J. Zhang, L. Li, Y. Peng, Y. Chen, X. Lv, S. Li, X. Qin, H. Yang, C. Wu, Y. Liu, Surface chemistry induces mitochondria-mediated apoptosis of breast cancer cells via PTEN/PI3K/AKT signaling pathway, Biochim Biophys Acta Mol Cell Res 1865(1) (2018) 172-185.

[42] T.A. Ulrich, E.M. de Juan Pardo, S. Kumar, The mechanical rigidity of the extracellular matrix regulates the structure, motility, and proliferation of glioma cells, Cancer Res 69(10) (2009) 4167-74.

[43] R. Mayor, S. Etienne-Manneville, The front and rear of collective cell migration, Nat Rev Mol Cell Biol 17(2) (2016) 97-109.

[44] T. Yeung, P.C. Georges, L.A. Flanagan, B. Marg, M. Ortiz, M. Funaki, N. Zahir, W. Ming, V. Weaver, P.A. Janmey, Effects of substrate stiffness on cell morphology, cytoskeletal structure, and adhesion, Cell Motil Cytoskeleton 60(1) (2005) 24-34.

[45] D.H. Kim, P.K. Wong, J. Park, A. Levchenko, Y. Sun, Microengineered platforms for cell

ACCEPTED MANUSCRIPT

mechanobiology, Annu Rev Biomed Eng 11 (2009) 203-33.

[46] C.H. Lee, D.D. Dershaw, D. Kopans, P. Evans, B. Monsees, D. Monticciolo, R.J. Brenner, L. Bassett, W. Berg, S. Feig, E. Hendrick, E. Mendelson, C. D'Orsi, E. Sickles, L.W. Burhenne, Breast cancer screening with imaging: recommendations from the Society of Breast Imaging and the ACR on the use of mammography, breast MRI, breast ultrasound, and other technologies for the detection of clinically occult breast cancer, J Am Coll Radiol 7(1) (2010) 18-27.

[47] S.M. Azarin, J. Yi, R.M. Gower, B.A. Aguado, M.E. Sullivan, A.G. Goodman, E.J. Jiang, S.S. Rao, Y. Ren, S.L. Tucker, V. Backman, J.S. Jeruss, L.D. Shea, In vivo capture and label-free detection of early metastatic cells, Nat Commun 6 (2015) 8094.

[48] S.S. Rao, G.G. Bushnell, S.M. Azarin, G. Spicer, B.A. Aguado, J.R. Stoehr, E.J. Jiang, V. Backman, L.D. Shea, J.S. Jeruss, Enhanced Survival with Implantable Scaffolds That Capture Metastatic Breast Cancer Cells In Vivo, Cancer Res 76(18) (2016) 5209-18.

[49] W.T. Arthur, L.A. Petch, K. Burridge, Integrin engagement suppresses RhoA activity via a c-Src-dependent mechanism, Curr Biol 10(12) (2000) 719-22.

[50] H. Yamaguchi, J. Condeelis, Regulation of the actin cytoskeleton in cancer cell migration and invasion, Biochim Biophys Acta 1773(5) (2007) 642-52.

[51] S.V. Plotnikov, C.M. Waterman, Guiding cell migration by tugging, Curr Opin Cell Biol 25(5) (2013) 619-26.

[52] A. Zemel, F. Rehfeldt, A.E. Brown, D.E. Discher, S.A. Safran, Optimal matrix rigidity for stress fiber polarization in stem cells, Nat Phys 6(6) (2010) 468-473.

[53] S. Suresh, Nanomedicine: elastic clues in cancer detection, Nat Nanotechnol 2(12) (2007)

ACCEPTED MANUSCRIPT

748-9.

[54] F. Chowdhury, S. Na, D. Li, Y.C. Poh, T.S. Tanaka, F. Wang, N. Wang, Material properties of the cell dictate stress-induced spreading and differentiation in embryonic stem cells, Nat Mater 9(1) (2010) 82-8.

[55] V. Swaminathan, K. Mythreye, E.T. O'Brien, A. Berchuck, G.C. Blobe, R. Superfine, Mechanical stiffness grades metastatic potential in patient tumor cells and in cancer cell lines, Cancer Res 71(15) (2011) 5075-80.

[56] W. Xu, R. Mezencev, B. Kim, L. Wang, J. McDonald, T. Sulchek, Cell stiffness is a biomarker of the metastatic potential of ovarian cancer cells, PLoS One 7(10) (2012) e46609.

[57] A. Kostic, C.D. Lynch, M.P. Sheetz, Differential matrix rigidity response in breast cancer cell lines correlates with the tissue tropism, PLoS One 4(7) (2009) e6361.

[58] M.F. Olson, E. Sahai, The actin cytoskeleton in cancer cell motility, Clin Exp Metastasis 26(4) (2009) 273-87.

[59] S. Kumper, F.K. Mardakheh, A. McCarthy, M. Yeo, G.W. Stamp, A. Paul, J. Worboys, A. Sadok, C. Jorgensen, S. Guichard, C.J. Marshall, Rho-associated kinase (ROCK) function is essential for cell cycle progression, senescence and tumorigenesis, Elife 5 (2016) e12994.

[60] R. Priya, X. Liang, J.L. Teo, K. Duszyc, A.S. Yap, G.A. Gomez, ROCK1 but not ROCK2 contributes to RhoA signaling and NMIIA-mediated contractility at the epithelial zonula adherens, Mol Biol Cell 28(1) (2017) 12-20.

[61] A. Yoneda, H.A. Multhaupt, J.R. Couchman, The Rho kinases I and II regulate different aspects of myosin II activity, J Cell Biol 170(3) (2005) 443-53.

[62] F.E. Lock, K.R. Ryan, N.S. Poulter, M. Parsons, N.A. Hotchin, Differential regulation of

ACCEPTED MANUSCRIPT

adhesion complex turnover by ROCK1 and ROCK2, PLoS One 7(2) (2012) e31423.

ACCEPTED MANUSCRIPT

Figures and Figure Legends

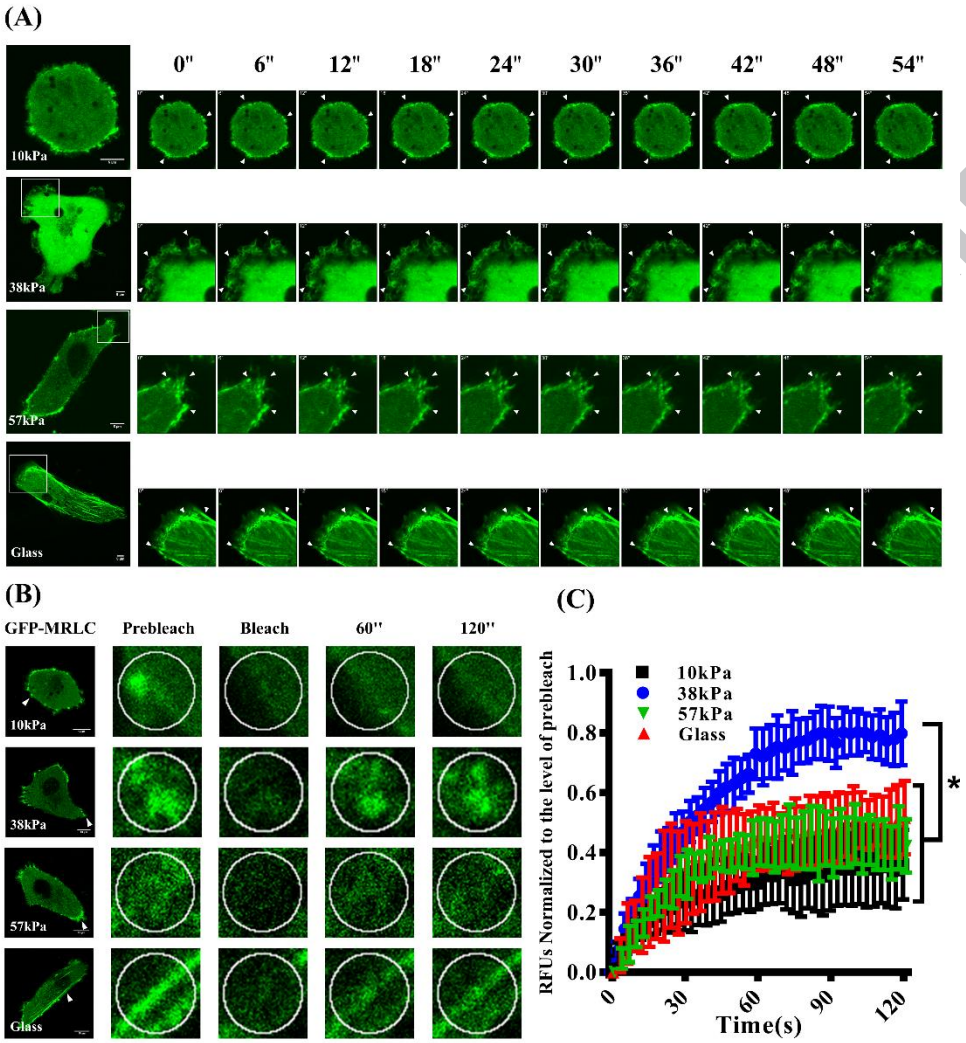

Fig. 1. Stiff substrates facilitate cytoskeletal dynamics in MDA-MB-231 cells. PAA gels with elastic modulus values of 10 kPa, 38 kPa, and 57 kPa were denoted as soft, stiff, and rigid, respectively. We used glass cell culture substrate as the control group and compared it with the PAA hydrogel cell culture substrate. (**A**) Cells were cultured onto substrates of different stiffness for 24 h and then transfected with GFP-MRLC to indicate cytoskeletal dynamics in membrane protrusion. Representative frames were cropped from living cells, and images in the left side show magnification of the white-boxed regions. Scale bar = 5 μm. (**B**) MDA-MB-231 cells cultured on substrates of different stiffness were subjected to FRAP analysis of GFP-MRLC in peripheral

ACCEPTED MANUSCRIPT

protrusions. Scale bar = 10 μm. (**C**) The graph shows the average mobile fraction fluorescence intensity in the bleached zone during recovery. Values are presented as mean ± SD of data from three independent experiments. *P<0.05.

ACCEPTED MANUSCRIPT

ACCEPTED MANUSCRIPT

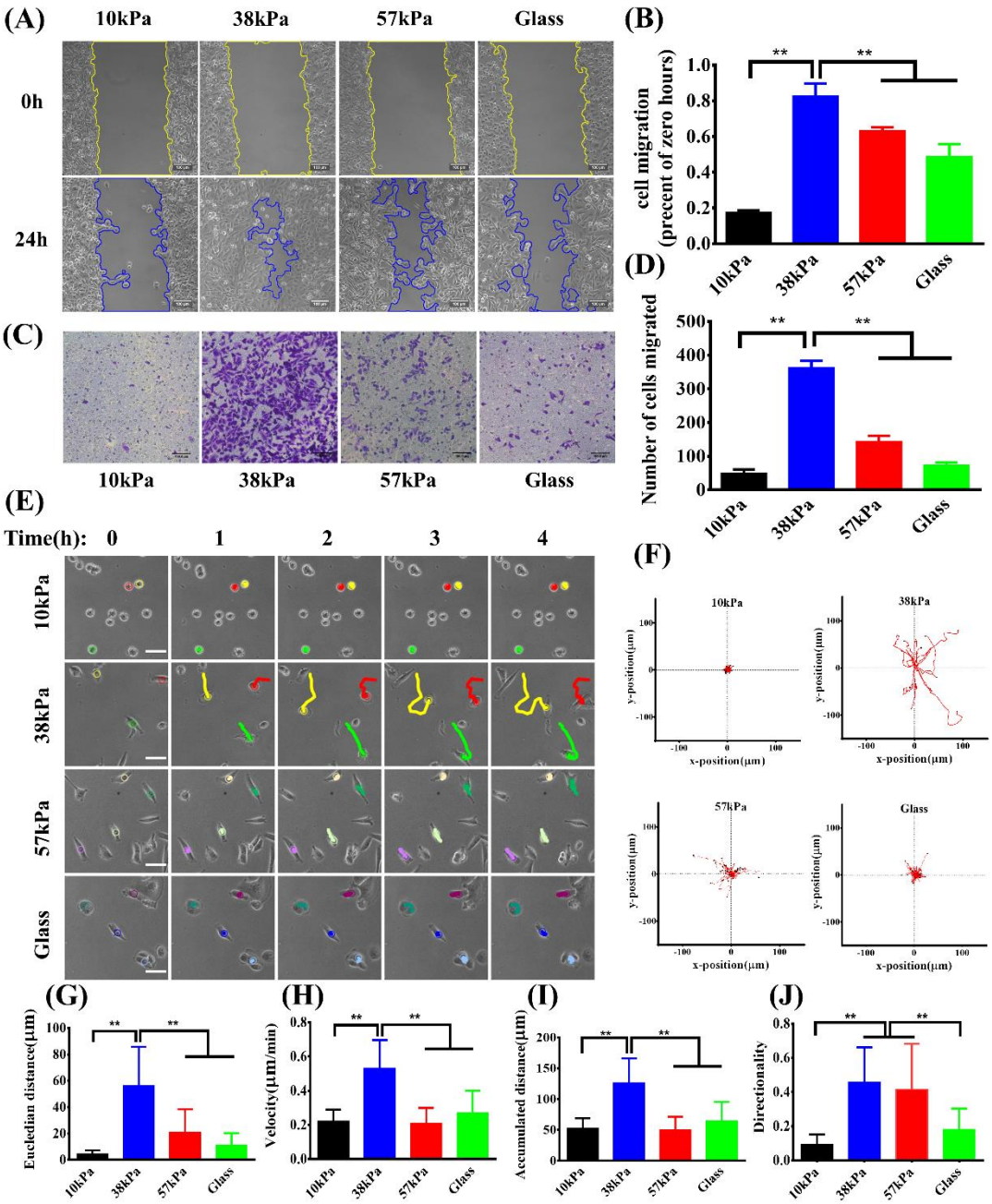

Fig. 2. Stiff substrates enhance cell motility in MDA-MB-231 cells. (**A**) Wound-healing assay of MDA-MB-231 cells was performed after cells were cultured on substrates of different stiffness for 48 h, and then the relative wound closure was observed under the microscope and photographed. Scale bar = 100 μm. (**B**) Quantification of the relative closure of scratch wounds was done by calculating the marked area in three randomly selected fields using ImageJ software, and the data are presented as mean ± SD. ***P*<0.01. (**C**) The cells were cultured on substrates of different stiffness for 48 h and then

ACCEPTED MANUSCRIPT

seeded into transwell culture inserts. After 12 h of culture, the cells on the upper side were removed, and the cells on the lower side were fixed and stained with crystal violet. Scale bar = 100 μm. (**D**) The cells that invaded the outer sides of the inserts were counted in five randomly selected fields and are presented as mean ± SD. ***P*<0.01. (**E**) Representative frames were cropped from living cells migration to show cell motility. MDA-MB-231 cells were cultured onto substrates of different stiffness for 48 h and immediately recorded by time-lapse microscopy for 4 h at 2-min intervals. Representative frames of 1 h intervals are presented for comparison. (**F**) Aggregated trajectories of individual cells are reported in (E). (**G-J**) A histogram reporting the Euclidean distance, average cell velocity, accumulated distance, and directionality of 50 cells cultured on substrates of different stiffness, respectively. Data are presented as mean ± SD. ***P*<0.01.

ACCEPTED MANUSCRIPT

ACCEPTED MANUSCRIPT

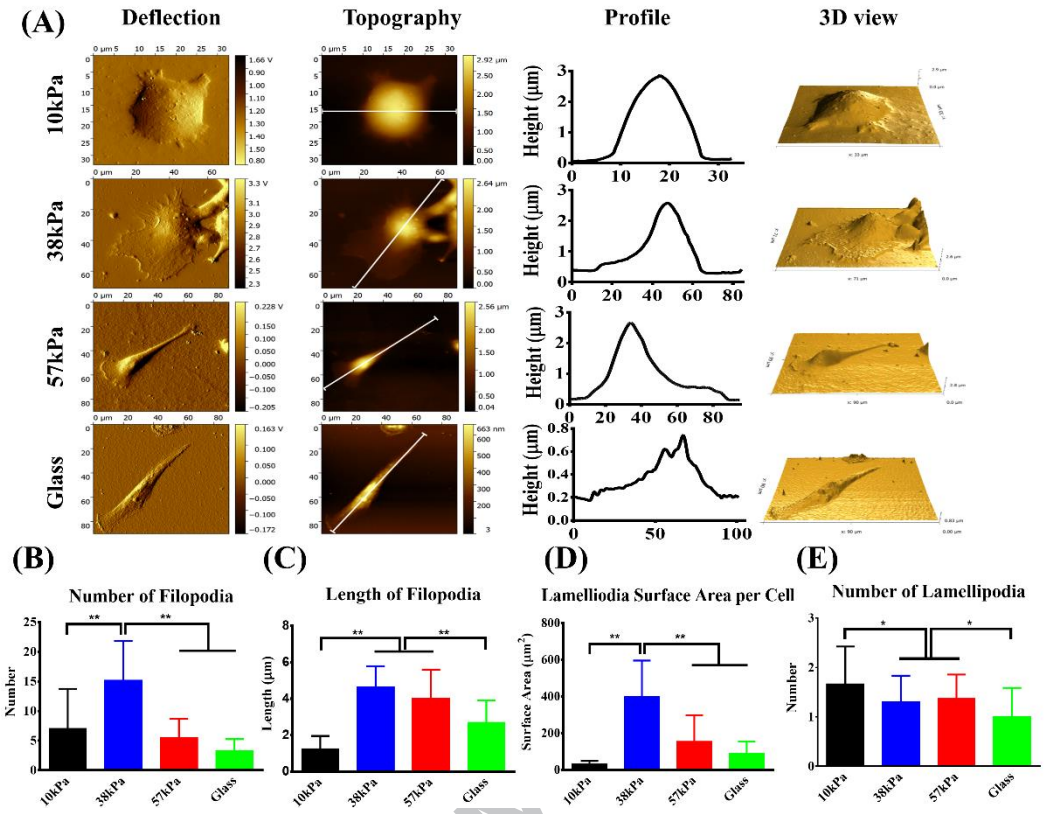

Fig. 3. Stiff substrates promote the formation of leading-edge protrusions observed by atomic force microscopy (AFM). (**A**) MDA-MB-231 cells were cultured on substrates of different stiffness for 48 h, and then AFM images were acquired. Deflection images reveal the cell membrane submicroscopic structures such as protrusions. Topographic images show the height of individual cells, and the profiles of cells were extracted from topographic images using ImageJ software (white segment on topographic images). 3D reconstitution of topography images was performed by Gwyddion. (**B-E**) Histograms showing the number of filopodia, length of filopodia, lamellipodia surface area per cell, and number of lamellipodia of 30 cells cultured on substrates of different stiffness, respectively. Data are presented as mean ± SD. **P*<0.05, ***P*<0.01.

ACCEPTED MANUSCRIPT

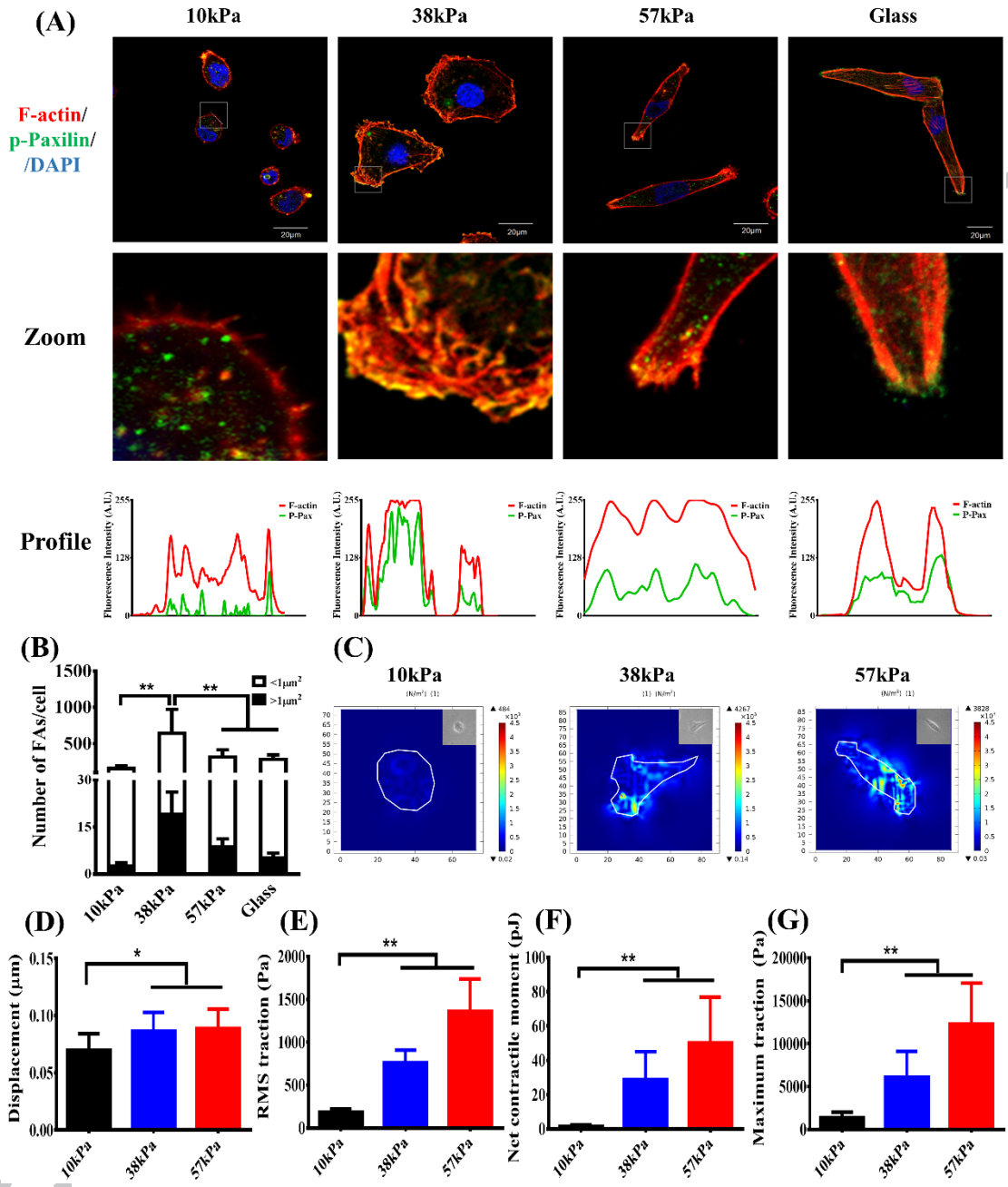

Fig. 4. Stiff substrates contribute to FA maturation and polarize traction force distributions in MDA-MB-231 cells. (**A**) Micrographs of FAs captured by confocal microscopy. MDA-MB-231 cells were cultured on substrates of different stiffness for 48 h and then immunostained for DNA (DAPI, blue), F-actin (phalloidin, red), and p-paxilin (FITC, green). Scale bar = 20 μm. Images in the lower row show magnification of the white boxed regions. Profiles of F-actin (red) and p-paxilin (green) were extracted from images (white segments) using ImageJ software. (**B**) From these images, the number

ACCEPTED MANUSCRIPT

of FAs per cell was calculated. Values are presented mean ± SD, n=30. **P<0.01. (**C**) MDA-MB-231 cells were cultured on substrates of different stiffness for 48 h, and then TFM was used to detect the magnitude and distribution of cell traction forces. White outlines define cell boundaries. Smaller panels show phase contrast micrographs of corresponding cells. (**D-G**) Histograms show the average displacement of fluorescent beads, RMS traction stresses, net contractile moment, and maximum traction of MDA-MB-231 cells cultured on substrates of different stiffness for 48 h. Data are presented as mean ± SD; the number of examined cells is 10. *P<0.05, **P<0.01.

ACCEPTED MANUSCRIPT

ACCEPTED MANUSCRIPT

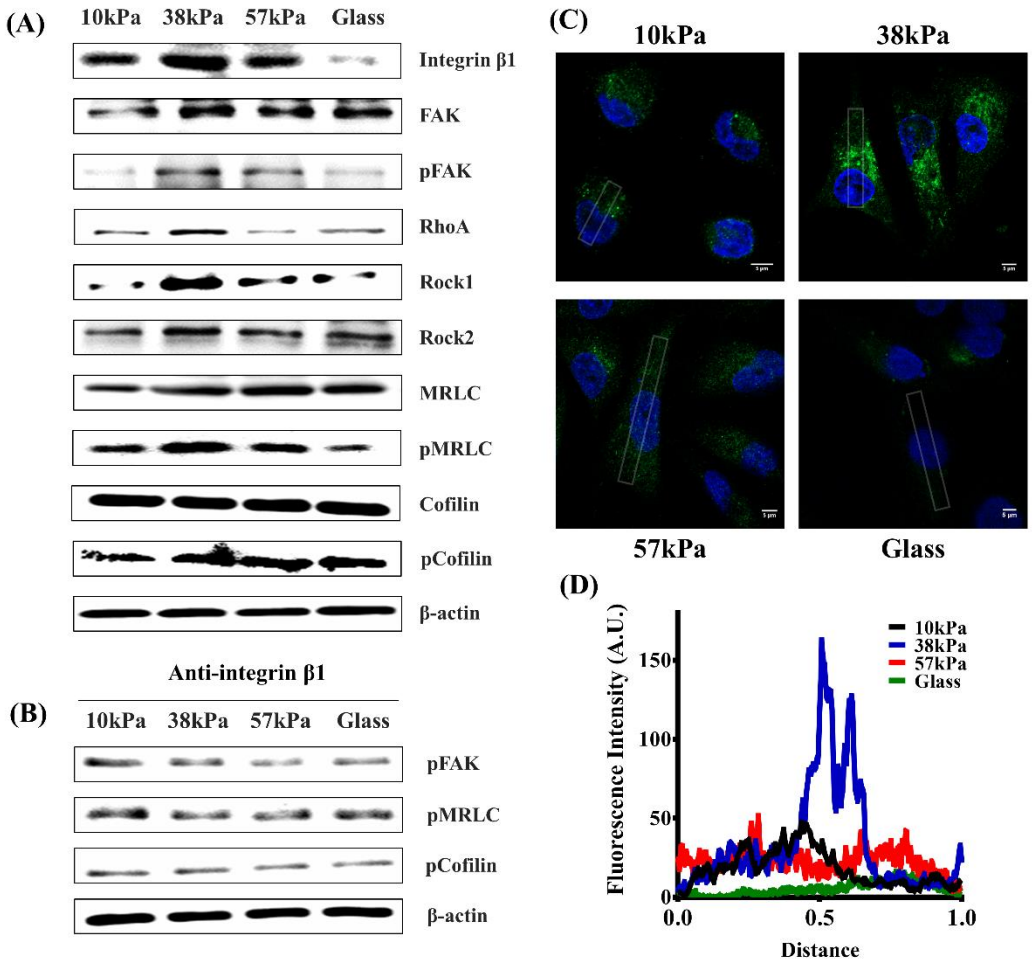

Fig. 5. Stiff substrates upregulate the protein expression and activation of RhoA, ROCK1, and ROCK2 signaling through integrin β1. (**A**) Cells were cultured on different substrates for 48 h, and then the expression of integrin β1, FAK, RhoA, ROCK1, ROCK2, MRLC, and cofilin was detected by western blotting. (**B**) After culturing for 48 h, the cells were treated with anti-integrin β1 antibodies for 6 h. Activation of FAK, MRLC, and cofilin was detected. (**C**) Active integrin β1 (FITC, green) in the cells was evaluated by immunofluorescence assay. Scale bar=5 μm. (**D**) The fluorescence intensity (A.U.) of the white-boxed regions in (C) was calculated using ImageJ software.

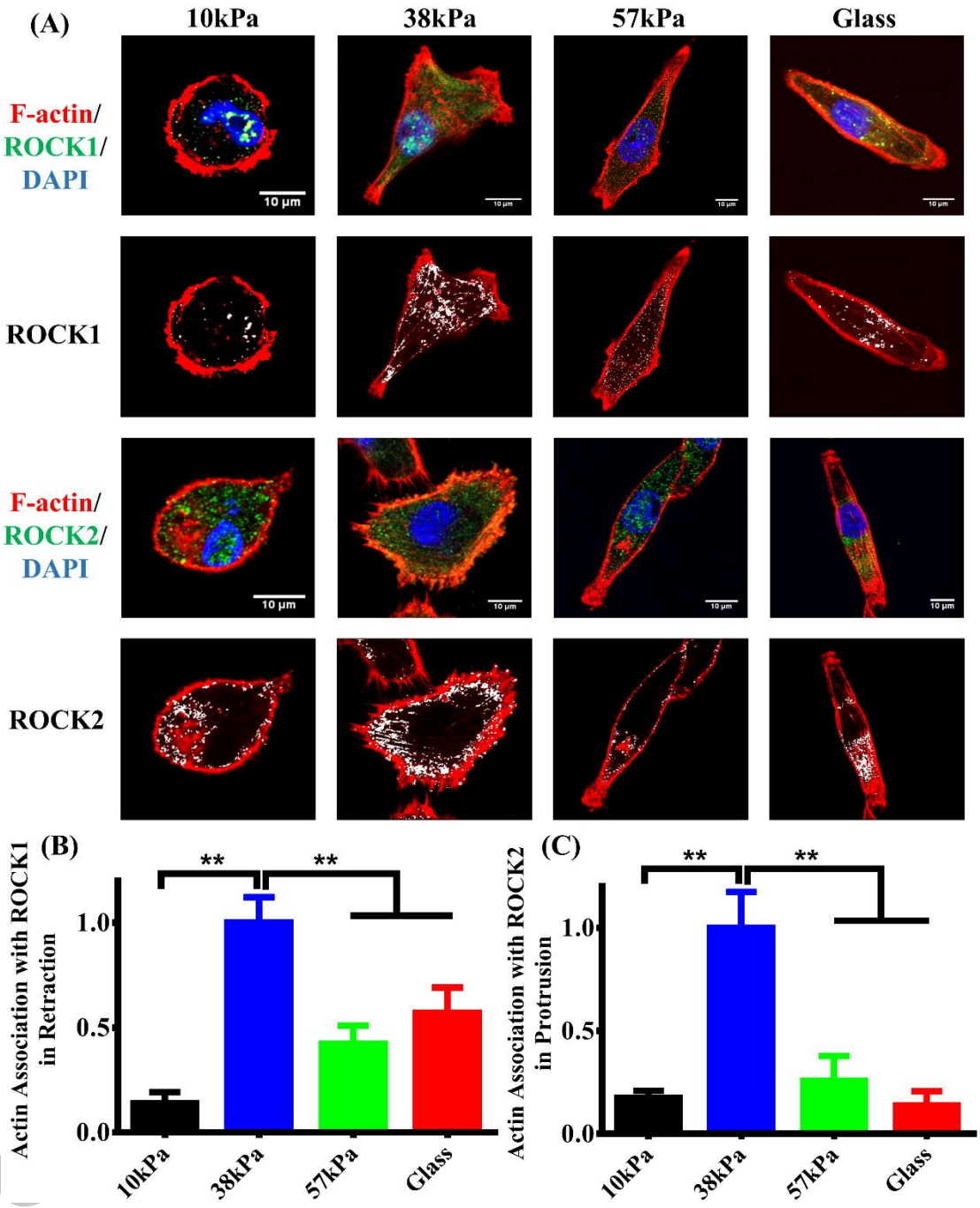

Fig. 6. ROCK1 preferentially localizes to actomyosin filament bundles, whereas ROCK2 localizes to membrane protrusions. (**A**) Representative MDA-MB-231 cells were cultured on substrates of different stiffness for 48 h, expressing either ROCK1 or ROCK2 (FITC, green) and containing DNA (DAPI, blue) and F-actin (phalloidin, red). Scale bar=10 μm. The white region of the cells in the lower row images shows that ROCK1 or ROCK2 colocalized with F-actin. (**B**) Quantification of the mean intensity of ROCK1 localized to F-actin

ACCEPTED MANUSCRIPT

in actomyosin filament bundles was determined. Values are presented as mean ± SD, n=10. **P<0.01. (**C**) Quantification of the mean intensity of ROCK2 localized to F-actin in protrusions was calculated. Values are presented as mean ± SD; n=10. **P<0.01.

ACCEPTED MANUSCRIPT

ACCEPTED MANUSCRIPT

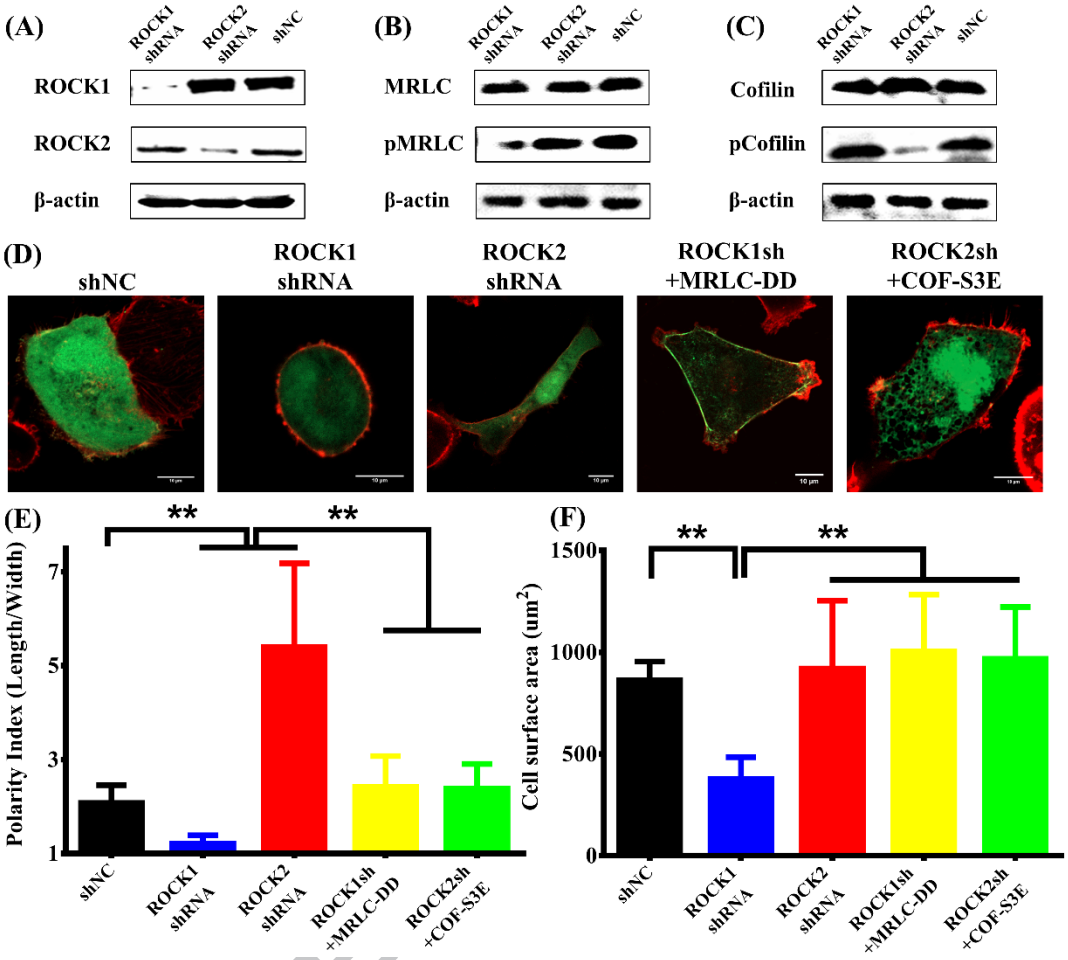

Fig. 7. ROCK1 and ROCK2 differentially phosphorylate MRLC and cofilin, thus regulating cell morphology through isoform-specific mechanisms. We used nontargeted shRNA as negative control (shNC) to compare with other treatments. (**A-C**) MDA-MB-231 cells were cultured on stiff substrates for 24 h and then transfected with ROCK isoform-specific shRNAs. After 48 h, the expression of ROCK1/ROCK2 and the phosphorylation of MRLC/cofilin were detected by western blotting. (**D**) These cells were immunostained for DNA (DAPI, blue) and F-actin (phalloidin, red) to indicate cell morphology. To confirm these results, MRLC-DD and COF-S3E were cotransfected with shRNAs. Scale bar = 10 μm. (**E-F**) Histograms showing the quantitative analysis of cell polarity indices and area were generated using ImageJ software. Values are presented as mean ± SD; n=15. ***P*<0.01.

ACCEPTED MANUSCRIPT

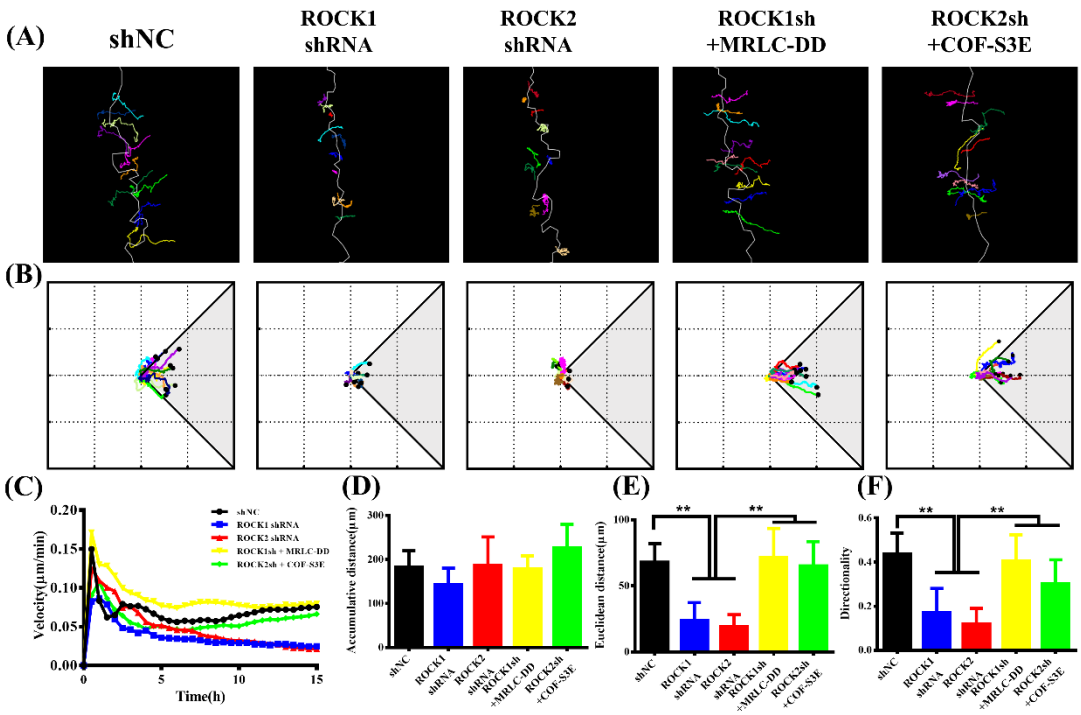

Fig. 8. MRLC and cofilin phosphorylation promotes directional migration of MDA-MB-231 cells. (**A**) MDA-MB-231 cells were cultured on stiff substrates for 24 h to grow as confluent monolayers and were transfected with ROCK isoform-specific shRNAs and/or plasmid mutants. Then, cell migration was recorded by time-lapse microscopy for 15 h after removing Ibidi-silicone inserts (Ibidi, Germany). Cell tracks were determined using ImageJ software, and the edge of the wound is indicated by a white line. Tracks of single cells at the wounded edge are shown. (**B**) Aggregated trajectories of individual cells are reported in A. Tracks that lie within a 90° angle with regard to the direction of cell movement were considered oriented (shaded region). (**C**) Instant velocity was analyzed for each cell type in A and is plotted as a function of time. (**D-F**) Histograms show the accumulated distance, Euclidean distance and directionality of each cell type; n=10. Data are presented as mean ± SD. $^{**}P<0.01$.

ACCEPTED MANUSCRIPT

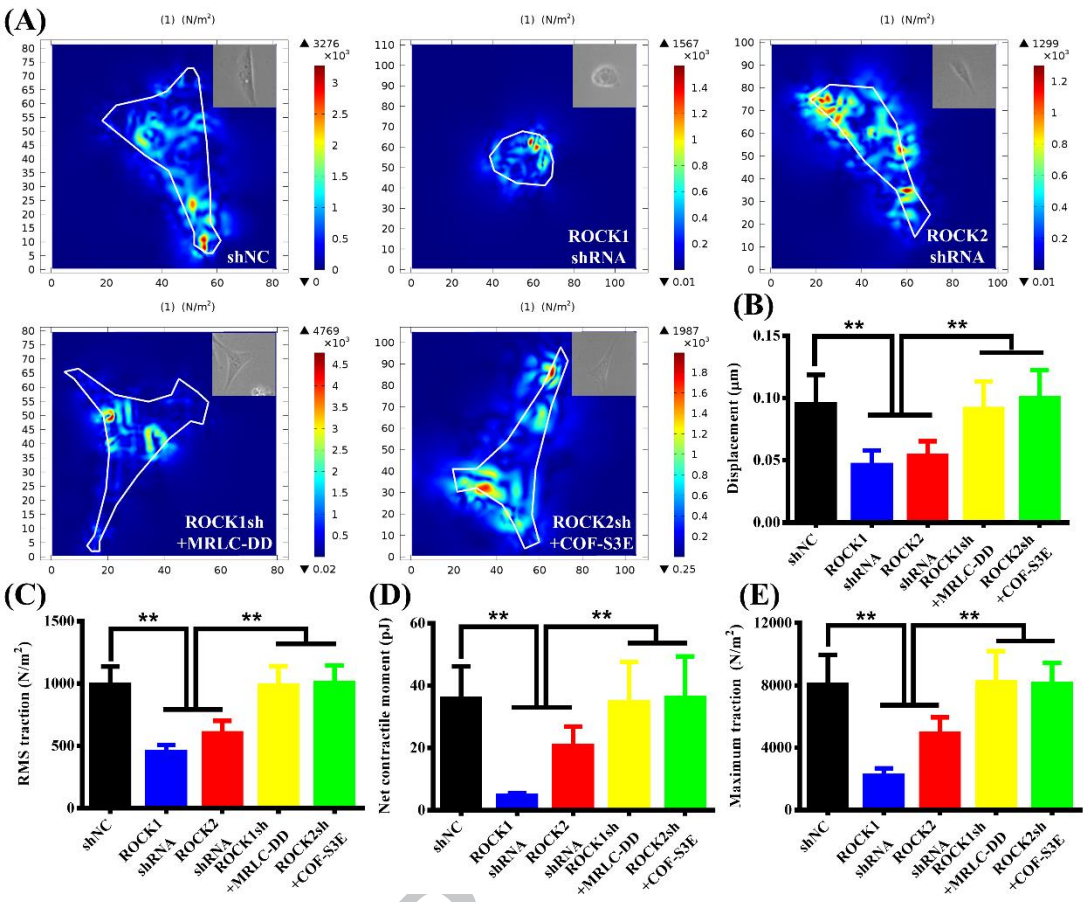

Fig. 9. MRLC and cofilin phosphorylation mediate the traction force generation and distribution. (**A**) MDA-MB-231 cells were cultured on stiff substrates for 24 h and then transfected with ROCK isoform-specific shRNAs and/or plasmid mutant. TFM was used to detect the magnitude and distribution of cell traction forces after 48 h. The white outline defines the cell boundary. Smaller panels show phase contrast micrographs of corresponding cells. (**B-E**) Histograms report the average displacement of fluorescent beads, RMS traction stresses, net contractile moment, and maximum traction of these 5 groups. Data are presented as mean ± SD; the number of examined cells was 10. ***P*<0.01.

ACCEPTED MANUSCRIPT

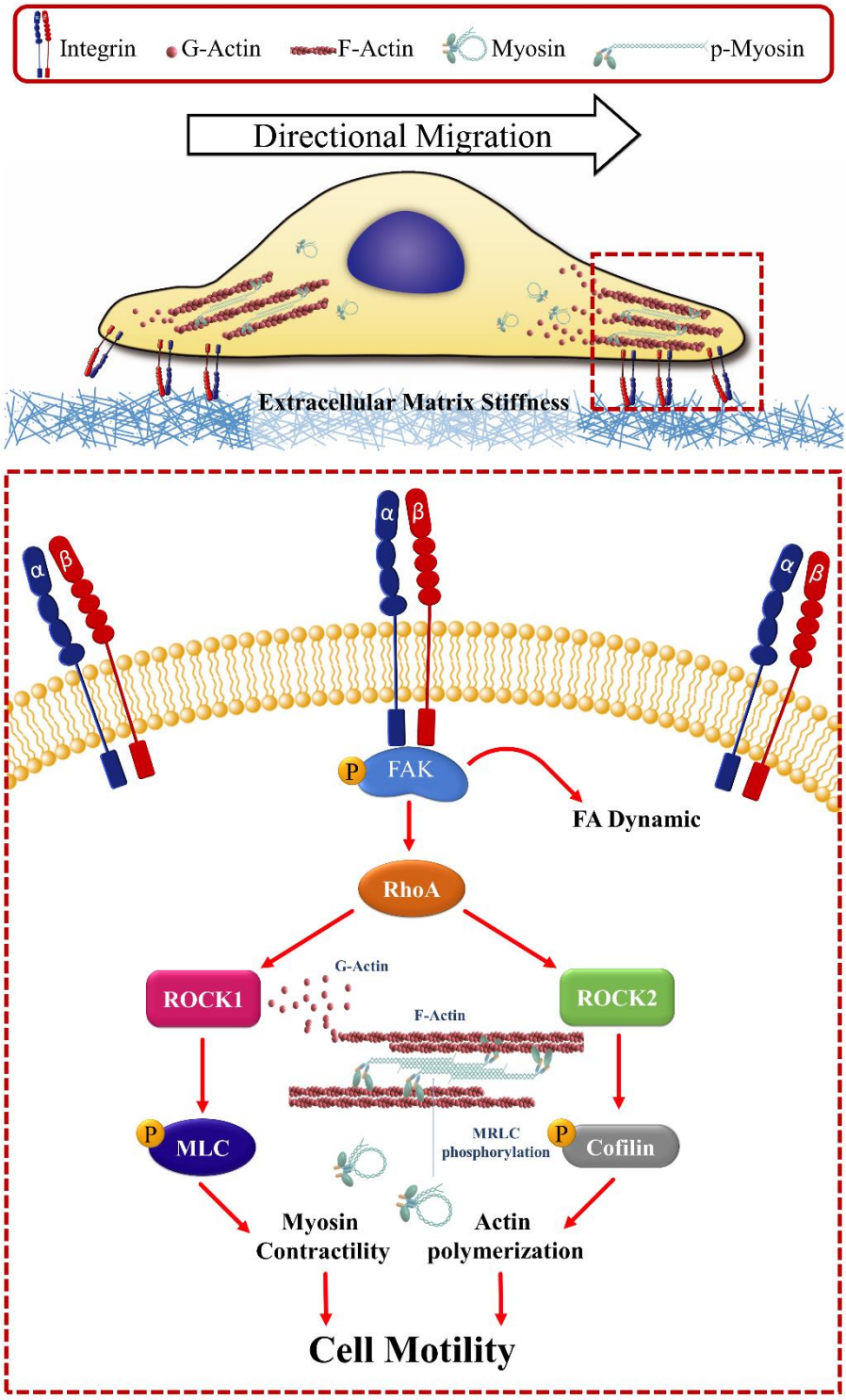

Fig. 10. Schematic illustration of the signaling pathway regulating MDA-MB-231 cell motility by mechanosensing the substrate stiffness. Extracellular matrix stiffness triggers multiple downstream events mediated directly by the expression and activation of integrin β1 and FAK. High FAK activity in cells cultured on stiff substrate upregulates RhoA expression.

ACCEPTED MANUSCRIPT

Subsequently, ROCK isoforms differentially promote actomyosin cytoskeleton rearrangement and synergistically regulate the extension of the lamellipodium at the front (right) of the migrating cell. Then, the activation of myosin-regulatory light chain contributes to detachment of the rear (left) of the moving cell.

Statement of significance

Here, we examined the relationship between substrate stiffness and tumor cellular motility by using polyacrylamide (PAA) substrates to simulate the stages *in vivo* of breast cancer. The results elucidated the different regulatory roles between the two ROCK isoforms in cell motility and demonstrated that stiff substrate (38kPa) mediated RhoA/ROCK1/p-MLC and RhoA/ROCK2/p-cofilin pathways through integrin β1-FAK activation and eventually promoted directional migration. Our discoveries would have significant implications in the understanding of the interaction between cancer cells and tumor microenvironments, and hence, it might provide new insights into the metastasis inhibition, which could be an adjuvant way of cancer therapy.

ACCEPTED MANUSCRIPT

ACCEPTED MANUSCRIPT

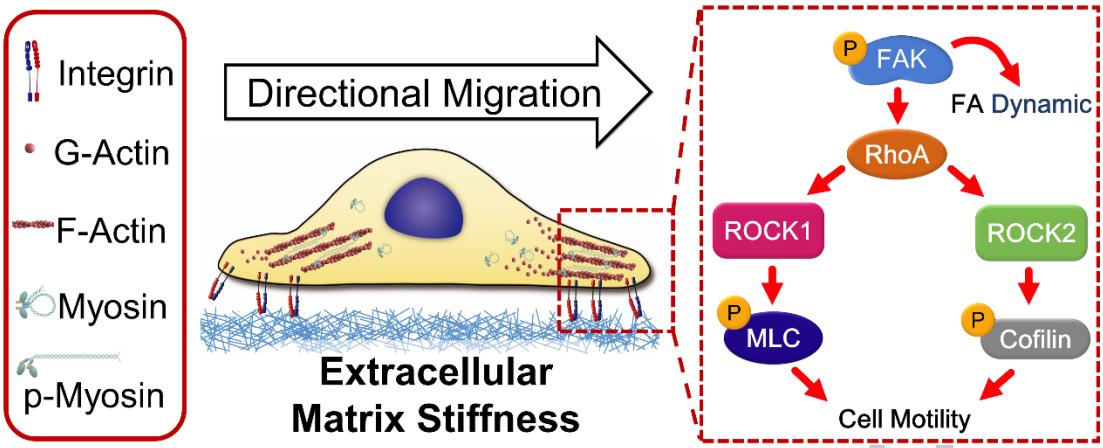

ACCEPTED MANUSCRIPT